Medical Physics
The International Journal of Medical Physics Research and Practice

Effect of improved TLD dosimetry on the determination of dose rate constants for 125I and 103Pd brachytherapy seeds

M. Rodriguez and D. W. O. Rogers

Citation: Medical Physics **41**, 114301 (2014); doi: 10.1118/1.4895003
View online: http://dx.doi.org/10.1118/1.4895003
View Table of Contents: http://scitation.aip.org/content/aapm/journal/medphys/41/11?ver=pdfcov
Published by the American Association of Physicists in Medicine

Effect of improved TLD dosimetry on the determination of dose rate constants for ^{125}I and ^{103}Pd brachytherapy seeds

M. Rodriguez[a)]
Carleton Laboratory for Radiotherapy Physics, Carleton University, Ottawa, Ontario K1S 5B6, Canada and Princess Margaret Hospital, Toronto, Ontario M5G 2M9, Canada

D. W. O. Rogers
Carleton Laboratory for Radiotherapy Physics, Carleton University, Ottawa, Ontario K1S 5B6, Canada

(Received 20 June 2013; revised 18 August 2014; accepted for publication 24 August 2014; published 17 October 2014)

Purpose: To more accurately account for the relative intrinsic energy dependence and relative absorbed-dose energy dependence of TLDs when used to measure dose rate constants (DRCs) for ^{125}I and ^{103}Pd brachytherapy seeds, to thereby establish revised "measured values" for all seeds and compare the revised values with Monte Carlo and consensus values.
Methods: The relative absorbed-dose energy dependence, f^{rel}, for TLDs and the phantom correction, P_{phant}, are calculated for ^{125}I and ^{103}Pd seeds using the EGSnrc BrachyDose and DOSXYZnrc codes. The original energy dependence and phantom corrections applied to DRC measurements are replaced by calculated $(f^{\mathrm{rel}})^{-1}$ and P_{phant} values for 24 different seed models. By comparing the modified measured DRCs to the MC values, an appropriate relative intrinsic energy dependence, $k_{\mathrm{bq}}^{\mathrm{rel}}$, is determined. The new P_{phant} values and relative absorbed-dose sensitivities, $S_{\mathrm{AD}}^{\mathrm{rel}}$, calculated as the product of $(f^{\mathrm{rel}})^{-1}$ and $(k_{\mathrm{bq}}^{\mathrm{rel}})^{-1}$, are used to individually revise the measured DRCs for comparison with Monte Carlo calculated values and TG-43U1 or TG-43U1S1 consensus values.
Results: In general, f^{rel} is sensitive to the energy spectra and models of the brachytherapy seeds. Values may vary up to 8.4% among ^{125}I and ^{103}Pd seed models and common TLD shapes. P_{phant} values depend primarily on the isotope used. Deduced $(k_{\mathrm{bq}}^{\mathrm{rel}})^{-1}$ values are 1.074 ± 0.015 and 1.084 ± 0.026 for ^{125}I and ^{103}Pd seeds, respectively. For (1 mm)^3 chips, this implies an overall absorbed-dose sensitivity relative to ^{60}Co or 6 MV calibrations of 1.51 ± 1% and 1.47 ± 2% for ^{125}I and ^{103}Pd seeds, respectively, as opposed to the widely used value of 1.41. Values of P_{phant} calculated here have much lower statistical uncertainties than literature values, but systematic uncertainties from density and composition uncertainties are significant. Using these revised values with the literature's DRC measurements, the average discrepancies between revised measured values and Monte Carlo values are 1.2% and 0.2% for ^{125}I and ^{103}Pd seeds, respectively, compared to average discrepancies for the original measured values of 4.8%. On average, the revised measured values are 4.3% and 5.9% lower than the original measured values for ^{103}Pd and ^{125}I seeds, respectively. The average of revised DRCs and Monte Carlo values is 3.8% and 2.8% lower for ^{125}I and ^{103}Pd seeds, respectively, than the consensus values in TG-43U1 or TG-43U1S1.
Conclusions: This work shows that f^{rel} is TLD shape and seed model dependent suggesting a need to update the generalized energy response dependence, i.e., relative absorbed-dose sensitivity, measured 25 years ago and applied often to DRC measurements of ^{125}I and ^{103}Pd brachytherapy seeds. The intrinsic energy dependence for LiF TLDs deduced here is consistent with previous dosimetry studies and emphasizes the need to revise the DRC consensus values reported by TG-43U1 or TG-43U1S1.
 [http://dx.doi.org/10.1118/1.4895003]

Key words: dose rate constants, LDR brachytherapy, EGSnrc, BrachyDose, TLD dosimetry, relative intrinsic energy dependence, relative absorbed-dose energy dependence

1. INTRODUCTION

Within the TG-43 formalism for brachytherapy dosimetry,[1,2] Λ, the dose rate constant (DRC) plays a central role since it relates the air-kerma strength of a seed, S_K to the dose rate 1 cm from the seed on its transverse axis, $D(1\text{ cm}, 90°)$ via

$$\Lambda = \frac{D(1\text{ cm}, 90°)}{S_K}. \tag{1}$$

All other dose rates around the seed are proportional to Λ. In general, as we show below, DRC measurements for ^{125}I (^{103}Pd) are systematically higher than Monte Carlo calculated Λ values by an average of 4.9% (4.1%) which led the AAPM TG-43 to define the DRC consensus value as the average of these two values. The measured values are almost universally dependent on measurements with LiF TLDs. The TLDs are irradiated in some sort of phantom and calibrated in terms of dose to water per unit reading in a ^{60}Co or 6 MV beam. The relative absorbed-dose sensitivity ($S_{\mathrm{AD,med}}^{\mathrm{rel}}$, formally defined below) of the TLD is then used to establish the equivalent dose to water per unit reading in the ^{125}I or ^{103}Pd field. This dose is the dose to water in the phantom material, and a phantom correction factor (P_{phant}, formally defined below) is used to derive the corresponding dose to water in water from the seed being investigated.

There are many uncertainties associated with the procedure. In the majority of measurement papers in the literature, a value of $S^{\mathrm{rel}}_{\mathrm{AD,med}} = 1.40$ or 1.41 was used based on a series of papers in the late 1980s and early 1990s.[3–8] The value of 1.4 was widely accepted as this is just the ratio of ratios of LiF to water mass energy absorption coefficients which is a simple theoretical expectation for the ratio in ^{60}Co and 20–30 keV (specifics below). There are several issues related to using these early values. For one, the shape of the TLD plays a significant role and, as we will show below, the $S^{\mathrm{rel}}_{\mathrm{AD,med}}$ values vary by 3%–4% from this issue alone and up to 8.4% when all issues are considered. Similarly, we will show that the simple model leading to a value of 1.40 is off by several percent due to absorption effects in the TLDs. Moreover, this simple model is actually only a model for the relative absorbed-dose energy dependence of the LiF, f^{rel}, i.e., the change in the ratio of the dose to the medium per unit dose to the LiF and not the required $S^{\mathrm{rel}}_{\mathrm{AD,med}}$. Finally, the measured values are all based on the state-of-the-art methods of dosimetry for the time, but since then, the primary standards and the dosimetry protocols used have all changed considerably.

In addition to the above issues, there is now clear evidence that the intrinsic energy dependence of LiF, i.e., the change in signal per unit dose to the LiF ($k^{\mathrm{rel}}_{\mathrm{bq}}$, formally defined below) varies by between 5% and 10% between ^{60}Co or 6 MV photon beams and the 20–30 keV photons in ^{125}I and ^{103}Pd dosimetry.[9–11] This further changes the expected value of $S^{\mathrm{rel}}_{\mathrm{AD,med}}$ although, as will be shown below, this tends to cancel some of the attenuation effects mentioned above.

The goal of this paper is to reanalyze the published values of measured DRCs making use of state-of-the-art Monte Carlo calculations of f^{rel}, the relative absorbed-dose energy dependence of the LiF detectors, and then determining the value of $k^{\mathrm{rel}}_{\mathrm{bq}}$, the intrinsic energy dependence of LiF, by determining the value which makes the measured values most closely agree with our Monte Carlo calculated values of the DRC. It will be shown that the value determined this way is consistent with the directly measured values. The paper then provides a revised set of DRCs for 24 different seed models and compares them to the previously recommended values from TG-43U1 (Ref. 2) or TG-43U1S1.[12]

Consistent with standard medical physics practice to date, we are ignoring the possible variation in the values of the intrinsic energy dependence of LiF detectors depending on the annealing and/or reading protocols followed. While not denying the potential impact of such variations which can be significant (see Refs. 13 and 14 and references therein), it is beyond the scope of this work to include this variable. Also, it is not explicitly corrected for in any of the experimental papers we have reanalyzed nor is there currently adequate knowledge to do so. It should be noted that the up to 3% difference between the measured results of $k^{\mathrm{rel}}_{\mathrm{bq}}$ in the recent literature[9,10] in the energy range of interest here has been attributed to being most likely due to different protocols although it could be due to different energy spectra or other reasons as well.

While the purpose of this paper is to reanalyze a large number of prior publication's values, we want to be clear that this is not meant as a criticism of these previous papers. In the majority of cases, these papers applied the state-of-the-art procedures and values that were available at that time. However, the field's knowledge and abilities to do calculations with much higher accuracy and statistical precision today make this reanalysis possible.

1.A. Formalism and notation

There is considerable confusion in the literature caused by varying terminologies, so it is essential to define a rigorous terminology, and we follow that used in Chap. 4 of the AAPM's 2009 Summer School book.[15] The absorbed-dose sensitivity of a detector is given by

$$S_{\mathrm{AD,med}} = \frac{M_{\mathrm{det}}}{D_{\mathrm{med}}} = \frac{1}{N_{D,\mathrm{med}}}, \tag{2}$$

where M_{det} is the detector's reading in the beam quality of interest with corrections made for effects such as for recombination, polarity, leakage, and dose rate dependencies, D_{med} is the dose to the phantom material (usually water) in the absence of the detector at the point of measurement (usually the midpoint of the detector) and $N_{D,w}$ is the absorbed-dose calibration coefficient for the detector in the beam quality of interest. The absorbed-dose sensitivity has two components. The first is f, the absorbed-dose energy dependence

$$f = \frac{D_{\mathrm{med}}}{\overline{D_{\mathrm{det}}}}, \tag{3}$$

where $\overline{D_{\mathrm{det}}}$ is the average dose to the detector's sensitive material. For low-energy beams, f is often approximated by the ratio of mass energy absorption coefficients

$$f \approx \left(\frac{\overline{\mu_{\mathrm{en}}}}{\rho}\right)^{\mathrm{med}}_{\mathrm{det}}. \tag{4}$$

The second component of $S_{\mathrm{AD,med}}$ is the intrinsic energy dependence of the detector, k_{bq} given by

$$k_{\mathrm{bq}} = \frac{\overline{D_{\mathrm{det}}}}{M_{\mathrm{det}}}. \tag{5}$$

These definitions lead to a simple relationship

$$D_{\mathrm{med}} = k_{\mathrm{bq}} f M_{\mathrm{det}}. \tag{6}$$

From these definitions we have

$$S_{\mathrm{AD,med}} = \frac{M_{\mathrm{det}}}{D_{\mathrm{med}}} = \frac{M_{\mathrm{det}}}{\overline{D_{\mathrm{det}}}} \frac{\overline{D_{\mathrm{det}}}}{D_{\mathrm{med}}} = \frac{1}{k_{\mathrm{bq}}} \frac{1}{f}. \tag{7}$$

Since TLDs are often calibrated in a high-energy photon beam, Q_o, for which the absorbed dose is known (usually ^{60}Co or 6 MV), and one needs the absorbed-dose sensitivity in a beam of quality Q, hence one needs the relative absorbed-dose sensitivity

$$S^{\rm rel}_{\rm AD,med} = \frac{S_{\rm AD,med}(Q)}{S_{\rm AD,med}(Q_o)} = \frac{k_{\rm bq}(Q_o)}{k_{\rm bq}(Q)}\frac{f(Q_o)}{f(Q)} = \frac{1}{k^{\rm rel}_{\rm bq}}\frac{1}{f^{\rm rel}}, \quad (8)$$

where the relative intrinsic energy dependence and relative absorbed-dose energy dependence are given by

$$k^{\rm rel}_{\rm bq} = \frac{k_{\rm bq}(Q)}{k_{\rm bq}(Q_o)}, \qquad f^{\rm rel} = \frac{f(Q)}{f(Q_o)}. \quad (9)$$

For relative absorbed-dose calibration coefficients one has (k_Q in TG-51 terminology[16])

$$N^{\rm rel}_{D,w} = \frac{N_{D,w}(Q)}{N_{D,w}(Q_o)} = k^{\rm rel}_{\rm bq} f^{\rm rel}. \quad (10)$$

The quantity $f^{\rm rel}$ can be calculated using Monte Carlo techniques and for photon detectors in low-energy beams is often approximated, following Eq. (4), as

$$f^{\rm rel} = \left[\left(\frac{\overline{\mu_{\rm en}}}{\rho}\right)^{\rm med}_{\rm det}\right]^{Q}_{Q_o}. \quad (11)$$

For TLDs in ^{125}I fields, the value of $f^{\rm rel}$ relative to a ^{60}Co beam is roughly 0.7 although the literature often deals with its inverse, viz., 1.4.

In Chap. 14 of the AAPM's 2009 Summer School book,[17] $f^{\rm rel}$ and $k^{\rm rel}_{\rm bq}$ were defined as the inverse of what is given in Eq. (9) above which is based on the definitions in Chap. 4 of the same book. Chap. 14 would be internally consistent except that it gives the same expression for calculating $f^{\rm rel}$ as in Eq. (11) above (i.e., Q over Q_o, see 2 lines above Eq. (14.20) in Chap. 14) and this is inconsistent with the definitions of Chap. 14. The equation for $k^{\rm rel}_{\rm bq}$ in that chapter (14.20) is also inconsistent with the expression for $S^{\rm rel}_{\rm AD,med}$ of Chap. 14. The remainder of this paper will use the quantities which are consistent with Chap. 4 definitions and as used elsewhere in the 2009 AAPM Summer School book.

Based on the Chap. 4 definitions and the relations derived above for the relative quantities, the final equations needed when measuring the value of the dose rate constant, Λ, are (ignoring linearity and phantom material effects, i.e., assuming a water phantom):

$$\Lambda = \frac{D_w}{S_K} = \frac{M_{\rm det}}{S_K\, S_{{\rm AD},w}} = \frac{M_{\rm det}}{S_K S^{\rm rel}_{{\rm AD},w} S_{{\rm AD},w}(Q_o)}, \quad (12)$$

$$= \frac{M_{\rm det} f^{\rm rel} k^{\rm rel}_{\rm bq}}{S_K S_{{\rm AD},w}(Q_o)}, \quad (13)$$

$$= \frac{M_{\rm det} f^{\rm rel} k^{\rm rel}_{\rm bq} N_{D,w}(Q_o)}{S_K}. \quad (14)$$

1.B. Literature values

1.B.1. k^{rel}_{bq}

Based on the information available at that time that $k^{\rm rel}_{\rm bq}$ was unity (albeit with large uncertainties),[18] some papers made the now known to be incorrect assumption that $S^{\rm rel}_{\rm AD}$ is numerically equal to $1/f^{\rm rel}$, but this ignores the relative intrinsic energy dependence of the detector, $k^{\rm rel}_{\rm bq}$. Many authors have demonstrated that at low energies $k^{\rm rel}_{\rm bq}$ for TLDs is not unity[9–11,13,19–21] with a value between 0.90 and 0.94 in the ^{125}I and ^{103}Pd energy range[9–11] (note that these papers present data for $1/k^{\rm rel}_{\rm bq}$ since they refer to an increase in the relative energy response which is basically $S^{\rm rel}_{\rm AD,med} \propto 1/k^{\rm rel}_{\rm bq}$). A value of $k^{\rm rel}_{\rm bq}$ less than unity means that the detector's reading per unit dose to the detector material is higher in the relevant beam quality than in the calibration beam. Using x-ray beam energies ranging from 20 to 250 kV(peak), Davis *et al.*[9] and Nunn *et al.*[10] determined that $1/k^{\rm rel}_{\rm bq}$ relative to ^{60}C, ranges from 1.08 to 1.11. Similarly, Tedgren *et al.*[11] reported values of 1.06–1.07 in this energy range.

1.B.2. $S^{rel}_{AD,med}$

While ignoring $k^{\rm rel}_{\rm bq}$ is incorrect for measurements of DRCs which are based on calculated $f^{\rm rel}$ values, nonetheless most of the DRC measurements to date have used values of the measured relative absorbed-dose sensitivity reported in the 1980s or early 1990s and thus, because they are measured, implicitly include $k^{\rm rel}_{\rm bq}$ values. Hartmann *et al.*[3] measured a ratio of TLD reading per unit dose to tissue, i.e., $S^{\rm rel}_{\rm AD,med}$, of 1.40 ± 2.8% for 40 kV(peak) x-rays relative to ^{60}Co photons. Weaver[4] found a TLD reading per unit dose to water of 1.39 ± 0.03 in the brachytherapy energy range relative to ^{60}Co. Later, Weaver *et al.*[5] found values of 1.47 ± 5% and 1.42 ± 5% for 6702 ^{125}I and 6711 ^{125}I seeds, respectively. Meigooni *et al.*[6,7] also reported a relative absorbed-dose sensitivity of 1.41 ± 3% for low-energy photon beams relative to a high-energy beam (4 MV). Muench *et al.*[8] also reported an $S^{\rm rel}_{\rm AD}$ value of 1.41 for 60 kV x-rays relative to 4 MV (3%–5% uncertainty estimated based on similar measurements[5,6,22,23]). The ratio of the mass energy absorption coefficient of LiF to water in the brachytherapy energy range relative to that at ^{60}Co is 1.41. Ignoring the need for the intrinsic energy dependence, the measured values are in good agreement with this simple theoretical expectation. As a result, a value of 1.40 or 1.41 has been generalized and used as the relative absorbed-dose sensitivity in many measurements of the DRC for the brachytherapy seeds currently in the market (see Tables IV and V below for individual values). However, it must be realized that all of these earlier reports on the value of $S^{\rm rel}_{\rm AD}$ were based on the TG-21[24] or similar protocols for the high-energy dosimetry, and the x-ray dosimetry was based on old protocols or procedures, often not specified. Furthermore, the high-energy measurements were usually based on the air kerma (formerly exposure) standards of the National Institute of Standards and Technology (NIST) for ^{60}Co and these have been revised.[25] In short, the measured value of 1.41 is based on many dosimetric quantities and procedures which have experienced changes, and the effects of these changes have not been tracked for their effect on this measured value, thereby making the proper value quite uncertain. In contrast, currently used measurements of dose rate constants are based on NIST's post-1999 S_K standard[26] and the TG-51[16] protocol for high-energy beam measurements. However, the values of the relative absorbed-dose sensitivity published in the articles mentioned above were often used to correct the TLD readings.

An exception to this trend is the recent work of Kennedy *et al.*[27] who explicitly accounted for a $k_{\mathrm{bq}}^{\mathrm{rel}}$ value of 0.916 ± 0.023 in their measurements of the DRC for the THINSeed 9011 and GE 6711 seed models. These measurements are not included in our analysis but compared to our results below.

1.B.3. f^{rel}

At low energies, TLD material attenuates photons more than water and hence, taking f to be the simple ratio of mass energy absorption coefficients as f is not applicable since the photon energy fluence is not the same in both materials. Mobit and Badragan[28] reported that for ^{125}I fields, Monte Carlo calculated values of f^{rel} relative to ^{60}Co vary between 1.32 and 1.41 for 5 and 1 mm diameter microrods. Calculation of the ratio of average attenuation and hence photon fluence between TLD and water for a detector x cm thick (i.e., $e^{-\mu_{\mathrm{TLD}}x/2}/e^{-\mu_w x/2}$) shows that for 2, 1, 0.4, and 0.1 mm thicknesses, the ratios are 0.930, 0.964, 0.986, and 0.996, respectively. Therefore, the finite thickness of the detector significantly affects the absorbed-dose energy dependence, f^{rel}, and consequently the measurement of the DRC of brachytherapy seeds.

1.C. Phantom corrections

Up to this point, the discussion has been about measurements and quantities defined in a water phantom, but for ^{125}I and ^{103}Pd seeds, almost all measurements are done in a plastic phantom of some sort. It is usually assumed that the relative absorbed-dose sensitivity of the TLDs, $S_{\mathrm{AD,med}}^{\mathrm{rel}}$, is unchanged when the measurement is in a phantom, despite the fact that the different phantom materials could cause the photon spectrum to be different at the location of the detector. Then, for a TLD calibrated at high energies in terms of absorbed dose to water, the TLD reading is thought of as reporting an absorbed dose to water, even when in a plastic phantom, i.e., the TLD is considered to be reporting D_w^{med}, the dose to water in the phantom medium. Hence, one measures $\Lambda_{\mathrm{med}} \equiv D_w^{\mathrm{med}}/S_K$. To extract the DRC in water, Λ_w, the phantom correction factor, P_{phant}, is defined such that

$$\Lambda_w = P_{\mathrm{phant}}\Lambda_{\mathrm{med}} \Rightarrow P_{\mathrm{phant}} = \Lambda_w/\Lambda_{\mathrm{med}} = D_w^w/D_w^{\mathrm{med}}, \tag{15}$$

where D_w^w is the dose to water at the reference point in a water phantom. Many papers have calculated Λ_{med} using Monte Carlo, shown it agreed with their measured value and then calculated Λ_w to allow calculation of P_{phant}. In other words, many measured values of Λ_w are actually directly proportional to a Monte Carlo calculated value of the same quantity, albeit in a ratio to Λ_{med}.

The statistical uncertainties on previous P_{phant} calculations are usually much higher than here, and hence we have systematically replaced them with our calculated values. However, as Patel *et al.*[29] have shown, variations in the actual composition of the phantom material, especially of the high-Z components, represent a significant potential uncertainty which is discussed below.

It is worth noting that TG-43U1 (Ref. 2) explicitly defined $E(r)$ to include the phantom correction factor, i.e., in our notation:

$$E(r) = \frac{S_{\mathrm{AD,med}}^{\mathrm{rel}}}{P_{\mathrm{phant}}} \tag{16}$$

$$= \frac{(f^{\mathrm{rel}})^{-1}}{P_{\mathrm{phant}}} \quad (\text{ignoring } k_{\mathrm{bq}}^{\mathrm{rel}}). \tag{17}$$

In a few papers it is actually used this way[29,30] but the much more common use has been $E(r) = S_{\mathrm{AD,med}}^{\mathrm{rel}}$ or $E(r) = (f^{\mathrm{rel}})^{-1}$ along with a separate assessment of P_{phant}. To further confuse the situation, in at least one paper[29] the calculated value of $E(r)$, based on Eq. (17), is said to "agree with previously published energy response measurements,[4,6,31]" whereas each of the papers cited measured $S_{\mathrm{AD,med}}^{\mathrm{rel}}$ (i.e., with no P_{phant} but including $k_{\mathrm{bq}}^{\mathrm{rel}}$).

2. METHODS

2.A. Relative absorbed-dose energy dependence and phantom correction

The relative absorbed-dose energy dependence is calculated as

$$f^{\mathrm{rel}} = \frac{(D_w/\overline{D_{\mathrm{TLD}}})_\gamma}{(D_w/\overline{D_{\mathrm{TLD}}})_{^{60}\mathrm{Co}}}, \tag{18}$$

where $\overline{D_{\mathrm{TLD}}}$ is the average absorbed dose in the TLD and D_w is the absorbed dose to water in a small voxel ($0.1\times0.1\times 0.05$ mm^3) at the midpoint of the detector in the absence of the detector. The numerator refers to values determined in the radiation field of interest and the denominator to those in the calibration beam. It is important not to use just the dose to water averaged over the detector volume as this averaging would decrease the value of f^{rel} by up to 2.4% due to $1/r^2$ effects, being more of an effect for larger detectors.

At brachytherapy energies the absorbed doses are calculated using BrachyDose, a fast EGSnrc-based[32,33] Monte Carlo code developed by Yegin *et al.*[34–36] to perform brachytherapy dose calculations. The voxel-based BrachyDose Monte Carlo calculations of TG-43U1 dosimetry parameters have been benchmarked by Taylor *et al.*[35] The absorbed dose to a TLD (D_{TLD}) is calculated in a LiF:MgTi $3\times3\times1$ mm^3 voxel centered at 1 cm from the axis of the seed on the transverse plane in a $30\times30\times30$ cm^3 water phantom. TLDs made of TLD-100 (LiF:MgTi) are the most commonly used detectors to measure the DRC. Consequently, the TLD material is simulated as LiF:MgTi material which has a fractional composition by weight of 0.26700 of lithium, 0.73279 of fluorine, 0.00020 of magnesium, and 0.00001 of titanium.[9] Since TLDs come in different sizes and forms, simulations are also performed using 6 mm long × 1 mm diameter rods or $1\times1\times1$ mm^3 cubes. These are the most common TLD sizes used in brachytherapy dose measurements. The rod's longitudinal axis is placed at 1 cm parallel to the longitudinal axis of the seed. The average dose to the detector is also calculated in TLDs with frontal areas of 3×3 mm^2 and 1×1 mm^2 and thicknesses of 0.8, 0.6, 0.4, and 0.1 mm. Several researchers[26,37–40] have demonstrated that ^{125}I seed models containing silver and those that are silver-free have notable differences in their generated spectra. Therefore, calculations were initially performed using three different sets of seeds: (a) ^{125}I seed models that contain silver components (GE Oncura 6711, Imagyn IS-12051, and MBI SL-125), (b) ^{125}I seed models that are silver-free (STM 1251, IBt 1251L, and Best 2301), and (c) ^{103}Pd seed models (Theragenics 200, MED3633, and Best 2335).

The phantom correction, Eq. (15), is calculated as the ratio of the dose to water in water [in a 1 mm^3 voxel] to the dose to water in phantom material[17] at the reference point (1 cm from the center of the seed on the transverse axis). In addition, it is also calculated as the ratio of the dose to TLD in water to the dose to TLD in phantom material at the reference point. Calculations were performed for the different phantom materials used in measurements, solid water[41] (SW), RW-1, also called plastic water,[42] or plastic water PW2030,[43] virtual water[44] (VW), PMMA and some reported variations on these materials. Table I gives the compositions used with the emphasis on the widely used RMI solid water for which several densities and compositions have been reported.[29,45]

When determining the $k_{\mathrm{bq}}^{\mathrm{rel}}$ in this work, the phantom correction (P_{phant}) used in TLD measurements is replaced by the new phantom correction ($P_{\mathrm{phant}}^{\mathrm{new}}$) calculated here.

Rayleigh scatter, bound Compton scatter, photoelectric absorption, and fluorescent emission of characteristic x-rays are included in the simulations. The photon energy cutoff is set to 1 keV with no electron transport. Photon cross-sections from the XCOM (Ref. 46) database are used in all calculations. One standard deviation statistical uncertainties are kept lower than 0.1%.

At high energy, $D_w/\overline{D_{\mathrm{TLD}}}$ is calculated using the EGSnrc DOSXYZnrc user code.[47] Dose is calculated in a LiF:MgTi $3\times3\times1$ mm^3 voxel on the central axis with the front face at depths of 2, 5, and 8 cm in a $30\times30\times30$ cm^3 water phantom. The dose ratio was also calculated for large and small chips and rods at 5 cm depth. The photon sources are a 10×10 cm^2 parallel ^{60}Co beam[48] and a 10×10 cm^2 parallel 6 MV Varian spectrum.[49] Simulation parameters are the same as for the low-energy simulations except that electron transport is simulated down to 10 keV (ECUT = 521 keV). One standard deviation statistical uncertainties are kept less than 0.1% in all high-energy simulations.

2.B. Relative intrinsic energy dependence

The inverse of the absorbed-dose energy dependence, $(f^{\mathrm{rel}})^{-1}$, found in this work is used to replace the ≈1.41 value of the relative absorbed-dose sensitivity used in many DRC measurements. As discussed above in Sec. 2.A, the finite size of the detector means it experiences a decreased dose compared to a point at the detector's midpoint on the axis. This is accounted for in our calculations and some authors have corrected for this effect[50–52] by increasing the TLD reading by a 1%–2% geometry correction where k_{geom} is the

TABLE I. Compositions and densities of phantom materials used in the calculations of P_{phant}. Values shown have considerable uncertainty and many values reported in the literature are just the manufactures stated values. Tello *et al.* (Ref. 61) reported spreads in density of 1.1%–4% for commercial phantom materials. Values are shown as originally reported but for the present calculations are renormalized to give 100%.

			Composition % by weight						
Phantom material	Reference	Density (g/cm^3)	H	C	N	O	Cl	Ca	Other
Water		0.998	11.2			88.8			
PMMA	Refs. 62 and 63	1.18 (ave)	8.0	60.0		32.0			
SW[a]	Ref. 64[b]	1.035	8.09	67.22	2.40	19.84	0.13	2.32	
SW[c]	Ref. 65[b]	1.015	8.09	67.22	2.40	19.84	0.13	2.32	
SWlowCa	Measured[29]	1.038 ± 0.8%	8.2	68.2	2.4	19.3	0.13	1.6	
SWmeas	Ref. 45	1.052	8.2	67.4	2.0	19.63	0.27	2.11	d
VW[e]	Ref. 44[b]	1.03[f]	8.02	67.03	2.14	19.9	0.14	2.31	
RW-1[g]	Refs. 42, 63, and 66	0.97	13.19	79.41		3.81		2.68	h
PW[i]	Refs. 61 and 64	1.014	9.25	62.82	1.0	17.94	0.96	7.95	j
PW2030	Ref. 43[k]	1.022	8.59	61.25	1.56	19.89	0.21		l

[a]SW is RMI-457, also called WT1.
[b]As reported by manufacturer.
[c]SW called RMI-451 in Ref. 65 but with lower density. Several papers cite this paper by Williamson for P_{phant} values.
[d]P 0.02, K 0.02.
[e]Virtual water: Refs. 41 and 62 give a slightly different composition.
[f]Ref. 67 measured 1.0467 g/cm^3.
[g]Often referred to as plastic water in the literature.
[h]Mg 0.91.
[i]Plastic water used in high-energy beams.
[j]0.03% Br.
[k]Values from Ref. 104 are within 0.01%.
[l]8.44% Al.

dose to the point on the detector's axis vs the dose averaged over the detector's volume. Thus, when the value of this correction was reported, we have taken it into account by dividing the reported $S^{\mathrm{rel}}_{\mathrm{AD,med}}$ value. Similarly, the value of P_{phant} determined in this work is used to replace the values used in the original work. This gives

$$\Lambda_{\mathrm{nok_{bq}}} = \Lambda_{\mathrm{reported}} (f^{\mathrm{rel}})^{\mathrm{present}} \frac{\left(S^{\mathrm{rel}}_{\mathrm{AD,med}}\right)^{\mathrm{reported}}}{k_{\mathrm{geom}}} (P_{\mathrm{phant}})^{\mathrm{present}}_{\mathrm{reported}}, \tag{19}$$

which deliberately ignores the relative intrinsic energy dependence, $k^{\mathrm{rel}}_{\mathrm{bq}}$. A global value of $k^{\mathrm{rel}}_{\mathrm{bq}}$ is determined by scaling $\Lambda_{\mathrm{nok_{bq}}}$ by $k^{\mathrm{rel}}_{\mathrm{bq}}$ as required by Eq. (13) or (14) and then minimizing the difference between the calculated and adjusted measured values doing a least squares fit varying $k^{\mathrm{rel}}_{\mathrm{bq}}$. Although this case is linear, the value of $k^{\mathrm{rel}}_{\mathrm{bq}}$ is determined using a graphical method for assigning uncertainties to parameters in nonlinear least squares fittings.[53] The χ^2 is given by

$$\chi^2(k^{\mathrm{rel}}_{\mathrm{bq}}) = \sum_{i=1}^{l} \frac{\Delta_i^2(k^{\mathrm{rel}}_{\mathrm{bq}})}{s^2_{m,i} + s^2_{c,i}}, \tag{20}$$

where $s_{m,i}$ and $s_{c,i}$ are the absolute uncertainties in the ith of l measurements and calculations, respectively, and Δ_i is

$$\Delta_i(k^{\mathrm{rel}}_{\mathrm{bq}}) = \Lambda_i(\mathrm{calculated}) - k^{\mathrm{rel}}_{\mathrm{bq}} \cdot \Lambda_{\mathrm{nok_{bq}}}(\mathrm{measured}). \tag{21}$$

The calculated values of Λ_i are those from column RR (Ref. 40) in Table VI discussed below.

In both previous calculations of Λ_i,[40,54] the statistical component of uncertainty was 0.3% or better. However, when calculating $k^{\mathrm{rel}}_{\mathrm{bq}}$ in Eqs. (20) and (21), $s_{c,i}$ also includes Type B uncertainties as recommended by AAPM TG-43U1/U1S1 (Refs. 2 and 12) for Monte Carlo simulations. Type B uncertainties include those generated by uncertainties from initial photon cross-section libraries, seed geometries, and photon energy spectra, whereas Type A uncertainties come from estimates of the statistical uncertainty inherent in the Monte Carlo technique. Type B uncertainty values are assigned based on various studies. Williamson[55] found that shifting of internal components of the ^{125}I Draximage LS-1 caused a DRC uncertainty of less than 2%. Dolan *et al.*[30] reported a total uncertainty of 0.75% due to geometry uncertainties of the Oncura 6711 seed model. As a compromise between the two previous values, the current work assigns an uncertainty of 1.2% to the DRCs due to geometric uncertainties. In a recent article,[40] we showed there is a negligible effect on the calculation of air kerma, dose and DRC for ^{125}I and ^{103}Pd full seed models when using any of four different initial spectra. AAPM TG-43U1 recommends an uncertainty of 0.1% due to uncertainty in the initial energy spectrum and that is conservatively adopted here. Uncertainty in the TG-43U1 parameters due to uncertainties in the photon cross-section libraries has been investigated by others (Bohm *et al.*,[56] DeMarco *et al.*,[57] Hedtjärn *et al.*,[58] Nunn *et al.*[10]). EGSnrc BrachyDose uses the NIST XCOM database, a current state-of-the-art photon cross-section library. Nunn *et al.*[10] reported an uncertainty of 0.86% on the calculated value of $(f^{\mathrm{rel}})^{-1}$ in this energy region due to cross-section uncertainties. We have adopted this value. Overall the total uncertainty assigned to the Monte Carlo calculated DRCs ($s_{c,i}$) is 1.5%. This value is lower than the generic uncertainty value of 2.5% suggested by AAPM TG-43U1 for DRCs calculated by Monte Carlo mainly because of the lower value assigned to the photoionization cross-section and seed geometry uncertainties (0.9% and 1.2% compared to the 1.5% and 2.0%, respectively, in TG-43U1). These lower values are assigned based on recent studies[10,30] not available at the time AAPM TG-43U1 were published.

The uncertainties on the measured DRC values, $s_{m,i}$, are adjusted by subtracting in quadrature the reported uncertainties of the original relative absorbed-dose sensitivity and phantom correction from the reported total uncertainty due to the fact that the original values are replaced by the relative absorbed-dose energy dependence and phantom correction found in this work so that $k^{\mathrm{rel}}_{\mathrm{bq}}$ can be determined. The uncertainties on our calculated values of P_{phant} and $(f^{\mathrm{rel}})^{-1}$ are likewise added back in quadrature. As cited explicitly below in the tables, the experimental dose rate constant values have been taken from 10 articles for 7 different ^{103}Pd seed models and from 25 articles for 17 different ^{125}I seed models. When appropriate, the corrected values reported in the TG-43 updates are used.[2,12]

3. RESULTS

3.A. Relative absorbed-dose energy dependence

Table II shows $(f^{\mathrm{rel}})^{-1}$ for ^{125}I and ^{103}Pd seeds for various TLD shapes. In general, data show that the relative absorbed-dose energy dependence varies with the detector thickness in the brachytherapy energy range. The shape of the frontal face (toward the seed) of the detectors is also important when measuring dose delivered by brachytherapy seeds because there is a detector volume effect that needs to be considered when using TLDs to measure dose in the low energy brachytherapy range. Because the linear attenuation coefficient increases quickly at low energies (20–30 keV), the effect is even more notable for ^{103}Pd seeds compared to ^{125}I seeds. The ratio $(f^{\mathrm{rel}})^{^{103}\mathrm{Pd}(20.6\ \mathrm{keV})}_{^{125}\mathrm{I}(27.3\ \mathrm{keV})}$ for 1.0, 0.6, 0.4, and 0.1 mm thickness is 1.027, 1.019, 1.013, and 1.004, respectively, for the TLD with 1×1 mm^2 frontal area. The ratio of the average attenuations $(e^{-\mu_w x/2}/e^{-\mu_{\mathrm{TLD}} x/2})^{^{103}\mathrm{Pd}(20.6\ \mathrm{keV})}_{^{125}\mathrm{I}(27.3\ \mathrm{keV})}$ for the same thickness are 1.05, 1.029, 1.019, and 1.004, respectively. Values are slightly different because the simple equations have been applied for monoenergetic sources and account only for the primary dose deposition, whereas the Monte Carlo results include some dose from scattered photons in the chip [up to a 3.5% (2.0%) effect in a $3\times3\times1$ ($1\times1\times1$) mm^3 LiF TLD]. For small detectors, as the thickness of the detector reduces down to a thin detector, the attenuation effect is minimal and the value of $(f^{\mathrm{rel}})^{-1}$ approaches the ratio of the mass energy absorption coefficient of LiF to water relative to that at ^{60}Co. TLDs with thickness of 0.1 mm do not exist in the market but are used here to show the thickness dependency of the ratio. The detector volume effect with rods is more significant,

TABLE II. Inverse of the relative absorbed-dose energy dependence, $(f^{\mathrm{rel}})^{-1}$, for ^{125}I (GE 6711, IS-12051 and MBI SL-125 with silver and STM 1251, IBt 1251L, and Best 2301 without silver) and ^{103}Pd (Theragenics 200, MED3633, and Best 2335) seeds relative to ^{60}Co (D_w/D_{TLD} values are 1.202, 1.214, and 1.208 for large chips, small chips, and rods, respectively). $(f^{\mathrm{rel}})^{-1}$ values are the average of the three seeds for each group and the value in parenthesis is the absolute difference between the maximum and minimum $(f^{\mathrm{rel}})^{-1}$ over all seeds of that group. Statistical component of uncertainty on $(f^{\mathrm{rel}})^{-1}$ is ≤0.2%.

	^{125}I		
TLD	With silver $(f^{\mathrm{rel}})^{-1}$	Silver-free $(f^{\mathrm{rel}})^{-1}$	^{103}Pd $(f^{\mathrm{rel}})^{-1}$
Large chips	(0.009)	(0.003)	(0.023)
$3\times3\times1$ mm^3	1.365	1.372	1.317
$3\times3\times0.8$ mm^3	1.371	1.376	1.329
$3\times3\times0.6$ mm^3	1.377	1.381	1.342
$3\times3\times0.4$ mm^3	1.383	1.385	1.356
$3\times3\times0.1$ mm^3	1.391	1.392	1.378
Small chips	(0.006)	(0.003)	(0.013)
$1\times1\times1$ mm^3	1.397	1.403	1.360
$1\times1\times0.8$ mm^3	1.404	1.407	1.372
$1\times1\times0.6$ mm^3	1.410	1.412	1.384
$1\times1\times0.4$ mm^3	1.416	1.417	1.398
$1\times1\times0.1$ mm^3	1.426	1.425	1.420
Rods	(0.024)	(0.007)	(0.028)
1.0 mm diam × 6 mm	1.356	1.358	1.305
0.1 mm diam × 6 mm	1.380	1.378	1.361

Note: $(f^{\mathrm{rel}})^{-1}$ values presented in table are relative to ^{60}Co. To find $(f^{\mathrm{rel}})^{-1}$ relative to 6 MV, D_w/D_{TLD} values at high energy need to be replaced by 1.205, 1.219, and 1.211 for large chips, small chips, and rods, respectively.

because $1/r^2$ effects lead to a lower dose to the TLD material at the ends of the detector and consequently brings down the average dose in the detector divided by the dose to a small voxel of water at the central point of measurement compared with the same ratio for a $1\times1\times1$ mm^3 microcube detector.

Generally, for small chips, only small differences were observed in f^{rel} values for ^{125}I seeds within the silver group or within the silver-free group, but a difference of up to 0.5% exists between the two groups for small chips. Large chips and rods, on the other hand, show considerable variation between seeds in each group. The effect is more evident in ^{103}Pd seed models with seed to seed variations of up to 1% for even the small chips. The values in parenthesis in Table II represent the absolute difference between the maximum and minimum $(f^{\mathrm{rel}})^{-1}$ values for all seeds studied, not just the three presented in more detail. Palladium seeds have differences up to 0.023 which represents approximately 1.8% of $(f^{\mathrm{rel}})^{-1}$ for large chips. Due to these differences, $(f^{\mathrm{rel}})^{-1}$ values were calculated specifically for each ^{103}Pd seed model and for ^{125}I seed models that used rods for DRC measurements.

For both high-energy beams (^{60}Co and 6 MV), the calculated dose ratio (D_w/D_{TLD}) does not change as a function of depth. However, different values were observed for each TLD shape. D_w/D_{TLD} values for ^{60}Co are 1.202, 1.214, and 1.208 for large chips, microcubes and rods, respectively. The same ratios for 6 MV are 1.205, 1.219, and 1.211, respectively. Statistical uncertainty for each value is 0.14%.

The $(f^{\mathrm{rel}})^{-1}$ values in column 7 of Tables IV and V presented below correspond to the specific seed, TLD shape and calibration source (^{60}Co or 6 MV) used in each measurement.

In the analysis used here and used at least indirectly in all measurements in plastic phantoms, is the assumption that the value of f^{rel} is the same whether the TLD is in water or in a plastic phantom. We verified this directly for a solid water phantom, and although the dose to a small water volume at 1 cm from the seed decreased by 3.3% near an ^{125}I seed and by 3.8% near a ^{103}Pd seed, the ratio of $D_w^{\mathrm{SW}}/D_{\mathrm{TLD}}^{\mathrm{SW}}$ vs the ratio of D_w^w/D_{TLD}^w was constant within the 0.1% statistics of the calculation for both seeds, and similarly the ratios at 5 cm depth in a ^{60}Co beam stayed constant at better than the 0.1% statistics. Hence, the values of f^{rel} are basically identical in water or solid water and we assume the same for all plastic phantoms.

3.B. Phantom correction

Table III presents calculated results for the phantom correction factors, P_{phant}, for the various phantom materials used for measurements of DRCs. P_{phant} values are very similar for different ^{125}I seed models although values for ^{103}Pd are generally further from unity and show a greater spread in values for different models. For SW, a 1.5% change in density has about a 0.2% effect on P_{phant} for ^{125}I seeds but a 1% effect for ^{103}Pd seeds. More importantly, the SW with a measured reduction in the calcium content has a 4.7% lower value of P_{phant} for ^{125}I seeds and an 8.1% lower value for ^{103}Pd seeds, consistent with the ^{125}I results of Patel *et al.*[29]

Average values of P_{phant} in solid water (1.052 ± 0.003 for ^{103}Pd and 1.035 ± 0.001 for ^{125}I) are used in Tables IV and V. This narrow range of values for a given radioisotope compares to the range in the literature of 1.030–1.054 for ^{103}Pd and 1.031–1.05 for ^{125}I seeds, which is mostly due to less statistical precision in many of the prior values and justifies using the values calculated here. In the present analysis, we adopt the average values of P_{phant} from Table I and assign an uncertainty of 3% in recognition of the impact of the uncertainties in the composition.

At high energy, the ratios D_w^w/D_w^{SW} or $D_{\mathrm{TLD}}^w/D_{\mathrm{TLD}}^{\mathrm{SW}}$ are 1.002 ± 0.002, which implies that at high energies, both water and solid water provide similar scatter to the detector. Also, explicit calculations for several cases show that the phantom correction does not change with TLD shape.

3.C. Relative intrinsic energy dependence

Tables IV and V present the measured DRCs and their respective uncertainties as reported by the authors [or as updated by TG-43 (Refs. 2 and 12)] along with the phantom correction and the relative absorbed-dose sensitivity used with those measurements. Experimental data are based on the post-1999 S_K standard at NIST (Refs. 26 and 59) and TG-51 (Ref. 16) protocol for high-energy beam calibrations. The tables show the measured dose rate constants of 7 ^{103}Pd seeds models and 17 ^{125}I seed models. Columns 6 and 7 in Tables IV and V show the P_{phant} and $(f^{\mathrm{rel}})^{-1}$ values for each seed model used in the

TABLE III. Monte Carlo calculated P_{phant} values to correct doses measured at 1 cm from the seed in a given material to the corresponding dose at 1 cm in water. P_{phant} values are given for four seeds of each radioisotope to show typical variations with seed model. The statistical uncertainty is about 0.2%. The calculations for SW with different densities and compositions show that the systematic uncertainties dominate the P_{phant} values. Values from the literature are shown for comparison, but these are often not for specific seed models.

	P_{phant}							
Density	SW	SW	SWlowCa	RW1	PW2030	VW	PMMA	PW
(g/cm^2)	1.03	1.015	1.036	0.970	1.022	1.030	1.180	1.014
Pd-103								
Theragenics 200	1.051	1.042	0.959	0.993	1.007	1.052	0.838	2.13
Ibt 1032P	1.055	1.046	0.959	0.994	1.009	1.056	0.831	2.18
Best 2335	1.048	1.040	0.957	0.991	1.004	1.050	0.834	2.13
MED3633	1.055	1.046	0.961	0.996	1.007	1.056	0.836	2.15
Average	1.052	1.044	0.959	0.994	1.007	1.054	0.835	2.15
Stdev (%)	0.3	0.3	0.2	0.2	0.2	0.3	0.4	1.1
Literature		1.049 (Ref. 66)		1.010 (Ref. 66)		0.929[a] (Ref. 44)	0.833 (Ref. 66)	
I-125								
GE 6711 (Ag)	1.037[b]	1.034	0.984	1.009	1.010	1.038	0.894	1.51
SL-125 (Ag)	1.036	1.034	0.984	1.009	1.009	1.038	0.894	1.51
MED3631 (noAg)	1.034	1.032	0.987	1.011	1.009	1.034	0.901	1.44
I25.S06 (noAg)	1.034	1.031	0.988	1.011	1.009	1.034	0.903	1.43
Average	1.035	1.033	0.986	1.010	1.009	1.036	0.898	1.47
Stdev (%)	0.1	0.1	0.2	0.1	0.1	0.2	0.5	3.0
Literature	[c]		[d]	1.009 (Ref. 66)	[e]		0.899 (Ref. 30) 0.893 (Ref. 66)	

[a]0.984 by scaling a figure in Ref. 29.

[b]The VW value of Wang and Hertel (Ref. 44) seems suspect as VW is very close to SW in composition but their P_{phant} values differ considerably. This anomalous value means the revisions below in Table IV for the OptiSeed IBt 1032P seed are anomalous and revised DRCs are not included in the analysis.

[c]1.048 ± 3%,[68] 1.043 ± 3%,[65] 1.0315,[69] 1.043 ± 3%,[50] 1.044 ± 0.2%,[70] 1.033 ± 4.6%,[71] 1.05 Ref. 72 quoting Ref. 65 (cf. 1.043 and 1.041 above), 1.036 Ref. 73 citing Ref. 65 (cf 1.043 above).

[d]1.038 (Ref. 66), 1.041 (Ref. 65) explicitly for 6711.

[e]Wallace reported a value of 0.995[74] for the phantom correction for PW2030, and this was used in a series of related papers. In a private communication, it became clear that what they correctly used was, in our notation, $P_{phant} = (1/0.995)(1/0.996) = 1.009$, where the 0.996 factor is the required F_{med} factor to convert from PW2030 to water.

TABLE IV. Dose rate constant values ($\Lambda \pm s'_m$) of ^{103}Pd seed models measured with TLDs. Columns 3, 4, and 5 represent the phantom correction ($P_{phant} \pm s_p$), the phantom material, and the relative dose sensitivity ($S^{rel}_{AD} \pm s_m$) originally used in the measurements. The last two columns represent the new phantom correction (P^{new}_{phant}) and the absorbed-dose energy dependence [$(f^{rel})^{-1}$] calculated in this work. Λ values with two references show the original report, but the value is as updated in TG-43U1 (Ref. 2). The statistical component of uncertainty on our calculated TLD corrections is ≤0.2%.

Seed model (reference)[a]	TLD measurements $\Lambda \pm s'_m$ (cGy h^{-1} U^{-1})	TLD corrections			New TLD corrections	
		$P_{phant} \pm s_p$	Material	$S^{rel}_{AD} \pm s_m$[b]	P^{new}_{phant}	$(f^{rel})^{-1}$
Theragenics 200 (Refs. 75 and 76)	0.68 ± 8% (Refs. 2 and 77)	1.048 ± 3%	SW	1.41 ± 3%	1.052	1.359
NASI MED3633 (Refs. 60 and 78)	0.702 ± 4.8% (Refs. 2 and 79)	1.0235 ± 0.7%	RW1	1.41 ± 3%[c,d]	0.994	1.313
OptiSeed IBt 1032P (Refs. 44 and 80)[e]	0.675 ± 7.5% (Ref. 44)[d]	0.9287 ± 3%	VW	1.4 ± 5%	1.054	1.363
Best 2335 (Refs. 81 and 82)	0.69 ± 8% (Ref. 81)	1.031 ± 4.2%	SW	1.4 ± 5%	1.052	1.368
	0.71 ± 10% (Ref. 82)[d]	1.047 ± 3%	VW	1.41 ± 3%	1.054	1.363
Draximage Pd-1 (Refs. 83 and 84)	0.67 ± 7.7% (Ref. 83)	1.066 ± 4.3%	SW	1.4 ± 3%	1.052	1.369
	0.66 ± 8% (Ref. 84)	1.043 ± 3%	SW	1.41 ± 3%	1.052	1.369
Advantage IAPd-103 (Ref. 85)	0.7 ± 9% (Ref. 85)	1.0298 ± 4.2%	SW	1.4 ± 5%	1.052	1.368
Intersource IBT 1031L (Ref. 86)	0.7 ± 6.5% (Ref. 86)	1.054 ± 4.2%	SW	1.4 ± 5%	1.052	1.372

[a]References are for seed descriptions.

[b]Value measured back in the 1980s or early 1990s.

[c]TLD rods used in measurements. The others used TLD microcubes (1 × 1 × 1 mm^3).

[d]^{60}Co used at high energy. The others used 6 MV.

[e]The OptiSeed result is presented to show the discrepancy in P_{phant} values, which is the result of the original paper using [in notation of Eq. (15)] $P_{phant} = D^w_w/D^{med}_{TLD}$ rather than the needed D^w_w/D^{med}_w (Ref. 105), and this throws in doubt their measured DRC which is excluded from further analysis.

TABLE V. Same as Table IV except for ^{125}I seed models.

Seed model (reference)	TLD measurements $\Lambda \pm s'_m$ (cGy h^{-1} U^{-1})	TLD corrections $P_{phant} \pm s_p$	Mat.	$S_{AD}^{rel} \pm s_m$[a]	New TLD corrections P_{phant}^{new}	$(f^{rel})^{-1}$
With silver						
GE 6711 (Refs. 30 and 65)	0.971 ± 6.1% (Ref. 30)	0.899[b]	PMMA	1.42 ± 0.3%	0.898	1.403
Imagyn IS-12051 (Refs. 87 and 88)	0.92 ± 8% (Ref. 87)	1.048 ± 3%	SW	1.41 ± 5%[c]	1.035	1.403
	0.95 ± 10% (Ref. 88)	1.043 ± 3%	SW	1.41 ± 3%[c]	1.035	1.403
ProstaSeed SL-125 (Refs. 74 and 89)	0.9805 ± 5.5% (Refs. 12 and 74)[e,f]	1.009 ± 2%	PW2030	1.45 ± 5%[c,d]	1.009	1.353
EchoSeed 6733 (Refs. 90 and 91)	0.99 ± 8% (Ref. 91)	1.05 ± 3%	SW	1.41 ± 5%[c]	1.035	1.403
IsoAid IAI-125A (Refs. 69 and 92)	0.96 ± 5% (Ref. 92)[e,f]	1.009 ± 2%	PW2030	1.45 ± 5%[c,d]	1.009	1.378
	1.02 ± 9% (Ref. 69)	1.032 ± 4.2%	SW	1.4 ± 5%[c]	1.035	1.403
SelectedSeed 130.002 (Refs. 50 and 51)	0.938 ± 6.9% (Ref. 50)[e]	1.043 ± 2.8%	SW	1.4 ± 2% /1.025	1.035	1.372
	0.987 ± 7.8% (Ref. 51)[e]	1.043 ± 3%	SW	1.4 ± 5% /1.025	1.035	1.372
Implant Scie. 3500 (Ref. 93)	1.01 ± 6% (Ref. 94)[e,f]	1.009 ± 2%	PW2030	1.42 ± 5%[c]	1.009	1.359
IsoSeed B. I12.S17 (Refs. 95 and 96)	0.951 ± 4.6% (Ref. 95)[e]	1.043 ± 1.4%	SW	1.4 ± 2% /1.025	1.035	1.378
Theragenics AgX100 (Refs. 70 and 97)	0.995 ± 6.6% (Ref. 70)	1.044 ± 0.2%	SW	1.41 ± 5%[c]	1.035	1.403
PharmaSeed BT-125-1	0.928 ± 8% (Ref. 71)	1.033 ± 4.6%	SW	1.4 ± 5%[c]	1.035	1.403
(Refs. 71 and 92)	0.95 ± 7.4% (Ref. 92)[e,f]	1.009 ± 2%	PW2030	1.43 ± 3%[c]/1.025	1.009	1.378
Silver-free						
Draximage LS-1 (Refs. 55 and 98)	1.02 ± 7% (Ref. 98)	1.043 ± 3%	SW	1.41 ± 5%[c]	1.035	1.409
Symmetra I25.S06 (Refs. 29 and 58)	1.033 ± 6.4% (Ref. 29)[f]	—[g]	SW	1.402 ± 4%	—	1.403
GE 6702 (Ref. 99)	1.056 ± 6% (Ref. 2)	—	—	1.47 ± 5%[c,h]	—	1.409
NASI MED3631 (Refs. 52 and 100)	1.06 ± 5% (Ref. 100)[e,f]	1.033 ± 0.7%	RW1	1.43 ± 3%[c]	1.010	1.361
	1.083 ± 4.8% (Ref. 52)[i,f]	—	W	1.45 ± 5%[c,d]/1.014	—	1.372
Best 2301 (Refs. 72 and 73)	1.03 ± 8% (Refs. 2 and 72)	1.05 ± 3%	SW	1.4 ± 5%[c]	1.035	1.409
	1.02 ± 7% (Ref. 73)	1.036 ± 3%	SW	1.41 ± 3%[c]	1.035	1.409
STM 1251 (Refs. 45 and 101)	1.039 ± 7% (Ref. 101)	1.034 ± 3%	SW	1.41 ± 3%[c]	1.035	1.409
	1.07 ± 5.5% (Ref. 45)	0.986[b]	SW	1.368 ± 0.3%	0.959	1.409
InterSource IBt 1251L	1.047 ± 9% (Ref. 102)	1.033 ± 4%	SW	1.4 ± 5%[c]	1.035	1.409
(Refs. 102 and 103)	1.05 ± 7% (Ref. 103)	1.031 ± 4%	SW	1.41 ± 5%	1.035	1.409

[a]Divided by geometry correction as shown, if reported, as per Eq. (18).
[b]Value deduced from $E(1\text{ cm}, 90)^{water}_{PMMA}$.
[c]Value measured back in the 1980s or early 1990s. The other values were determined by Monte Carlo calculation and are actually $(f^{rel})^{-1}$ values since k_{bq}^{rel} was not accounted for or taken as unity.
[d]Authors cited Weaver *et al.* (Ref. 5) who reported two values. Average is used.
[e]TLD rods used in measurements.
[f]^{60}Co used at high energy. The others used 6 MV.
[g]P_{phant} included in published S_{AD}^{rel}.
[h]Energy response for model 6702 measured by Weaver *et al.* (Ref. 5).
[i]TLD large chips used in measurements. The others used TLD microcubes (1 × 1 × 1 mm^3).

determination of k_{bq}^{rel} in this work. Columns 2 and 3 in Table VI show the MC calculated dose rate constants for the same seed models. Both sets of Monte Carlo DRCs were calculated using the EGSnrc BrachyDose code and have similar values (but not always within the statistical component of uncertainty) except for two ^{125}I seed models (NASI MED3631 and STM1251) and three ^{103}Pd seed models (Theragenics, NASI MED3633, and IsoAid Advantage IAPd-103). Two of these seeds have recently had a revision in the geometry description of the seed in our database. The previous IAPd-103 seed model had a minor mistake in the geometry description (a small region near the seed had water instead of air in it) which was affecting the air-kerma calculation (but not the in-phantom calculations), and the NASI MED3633 geometry was modified and updated as described by Rivard.[60] Due to the loss of previous seed input files, it has not been possible to identify the reasons for DRC discrepancies for the other seeds. However, the revised measured values presented below are on average slightly closer to the calculated values in Ref. 40, which are used in the rest of the present analysis. Column 5 presents the $\Lambda_{nok_{bq}}$ value calculated using Eq. (18) and data in Tables IV and V. For seed models with two entries in Tables IV and V, $\Lambda_{nok_{bq}} \pm s''_m$ represents the average of the two values.

Figures 1 and 2 show plots of χ^2 as a function of the fitting parameter k_{bq}^{rel} [in Eq. (20)] for ^{125}I and ^{103}Pd seed models, respectively. The fitted k_{bq}^{rel} value is given at χ^2_{min} and the uncertainty is determined by taking the corresponding values at $\chi^2_{min}+1$ (Ref. 53). The $k_{bq}^{rel}((k_{bq}^{rel})^{-1})$ values are 0.931 ± 0.013 (1.074 ± 0.015) and 0.922 ± 0.022 (1.084 ± 0.026) for ^{125}I and ^{103}Pd seed models, respectively.

The relative intrinsic energy dependence deduced from the revised measured DRCs is reasonably consistent with values found by some other authors for x-ray beams[9–11] as shown in Fig. 3. The intrinsic energy dependence found in this work

TABLE VI. Dose rate constant values of ^{103}Pd seed models calculated using Monte Carlo simulation. MC calculations from Refs. 40 and 54 have statistical component of uncertainties of 0.3% or less. The TLD measurements column shows $\Lambda_{\mathrm{nok_{bq}}} \pm s''_m$ which is the modified measured DRC value with the original P_{phant} and $S^{\mathrm{rel}}_{\mathrm{AD}}$ values (columns 3 and 5 in Tables IV and V) replaced by the $P^{\mathrm{new}}_{\mathrm{phant}}$ and $(f^{\mathrm{rel}})^{-1}$ values calculated in this work (columns 6 and 7 in Tables IV and V), and the s''_m is the adjusted percentage uncertainty $s''_m = \sqrt{s'^2_m - s^2_m - s^2_P}$. The value of $\Lambda_{\mathrm{nok_{bq}}}$ deliberately ignores the intrinsic energy dependence, $k^{\mathrm{rel}}_{\mathrm{bq}}$. The last column represents the % difference between the Λ_{MC} (column RR) and $\Lambda_{\mathrm{nok_{bq}}}$.

	Dose rate constant Λ (cGy h^{-1} U^{-1})				
	MC calculation			TLD measurements	
Seed model	RR (Ref. 40)	TR (Ref. 54)	Diff%	$\Lambda_{\mathrm{nok_{bq}}} \pm s''_m$	$[(\Lambda_{\mathrm{nok_{bq}}} - \Lambda_{\mathrm{MC}})/\Lambda_{\mathrm{MC}}]\%$
^{103}Pd					
Theragenics 200	0.685	0.694	−1.3	0.708 ± 7.4%	3.4
NASI MED3633	0.665	0.650	2.2[a]	0.732 ± 4.7%	10.1
Best 2335	0.654	0.650	0.6	0.730 ± 7.5%	11.6
Draximage Pd-1	0.627	0.632	0.8	0.681 ± 6.9%	8.6
Advantage IAPd-103	0.661	0.687	−3.9[a]	0.732 ± 6.9%	10.7
InterSource IBT 1031L	0.663[c]	0.663	0.0	0.713 ± 3.1%	7.5
^{125}I					
GE 6711	0.928	0.924	0.4	0.983 ± 6.1%	5.9
Imagyn IS-12051	0.924	0.924	0.0	0.930 ± 7.9%	0.7
ProstaSeed SL-125	0.931	0.930	0.1	1.051 ± 3.2%	12.9
EchoSeed 6733	0.934	0.929	0.5	0.981 ± 6.2%	5.0
IsoAid IAI-125A	0.925	0.925	0.0	1.015 ± 5.7%	9.8
SelectSeed130.002	0.917	0.917	0.0	0.951 ± 6.1%	3.7
Implant Scie. 3500	0.987[b]	0.994	0.7	1.055 ± 4.0%	6.9
IsoSeed B. I12.S17	0.915[c]	0.916	−0.1	0.935 ± 4.9%	2.2
Theragenics AgX100	0.900[c]	n/a	n/a	0.991 ± 5.2%	10.1
PharmaSeed BT-125-1	0.906[c]	0.901	0.5	0.945 ± 6.2%	4.3
Draximage LS-1	0.922	0.922	0.0	1.013 ± 4.9%	9.9
Symmetra I25.S06	1.004[b]	1.011	0.7	1.032 ± 5.8%	1.9
GE 6702	1.007	1.000	0.7	1.102 ± 3.3%	9.4
NASI MED3631	0.995	0.978	1.7	1.109 ± 5.3%	11.4
Best 2301	0.999	0.998	0.1	1.014 ± 6.9%	1.5
STM 1251	0.992	1.012	−2.0	1.040 ± 6.3%	4.8
InterSource IBt 1251L	0.991	0.992	−0.1	1.049 ± 5.6%	5.8

[a]Seed models changed. See text.
[b]Values differ from Ref. 40 based on further seed model changes identified by Ref. 106.
[c]Dose rate constants calculated in this work.

applies directly to ^{125}I and ^{103}Pd seeds rather than to x-ray spectra as in most previous studies. Das *et al.*[18] reported a relative intrinsic energy dependence value of 1.0, but the reported uncertainties on those data were large. Values of Das *et al.* at ≈20 keV are not as consistent with ours as those at 28 keV, and their 20 keV values are even farther from the other previous results.[10,11]

3.D. Calculated vs revised measured dose rate constants

For each seed model, Table VII shows the Monte Carlo calculated DRC, Λ_{MC} (from column RR, Table VI), and the revised measured DRC, $\Lambda^{\mathrm{rev}}_{\mathrm{meas}}$, which is determined by replacing the phantom correction and relative absorbed-dose sensitivity used originally to determine the experimental values, by the new phantom correction and relative absorbed-dose sensitivity values, $S^{\mathrm{rel}}_{\mathrm{AD,med}} = (f^{\mathrm{rel}} \cdot k^{\mathrm{rel}}_{\mathrm{bq}})^{-1}$. The P_{phant} and $(f^{\mathrm{rel}})^{-1}$ values are taken from Tables IV and V, and the $(k^{\mathrm{rel}}_{\mathrm{bq}})^{-1}$ values are as determined above. After revising the measured DRCs, the average MC calculated values compared to measured values are 1.2% higher and 0.2% lower for ^{125}I and ^{103}Pd seeds, respectively. This compares with average calculated DRCs being 4.8% lower than the "as published" DRCs. For each seed model, the table also presents $\Lambda^{\mathrm{rev}}_{\mathrm{avg}}$, the average value of the revised measured DRC and the Monte Carlo calculated DRC, and the percentage difference between that average and the consensus value reported in TG-43U1 (Ref. 2) or TG-43U1S1 (Ref. 12). The consensus values are on average 3.8% and 2.8% higher than the average of the calculated and revised measured DRCs for ^{125}I and ^{103}Pd brachytherapy seeds, respectively.

Table VIII presents a comparison of our results for the THINSeed 9011 and GE 6711 to those of Kennedy *et al.*[27] who also properly took into account $k^{\mathrm{rel}}_{\mathrm{bq}}$. Our calculated

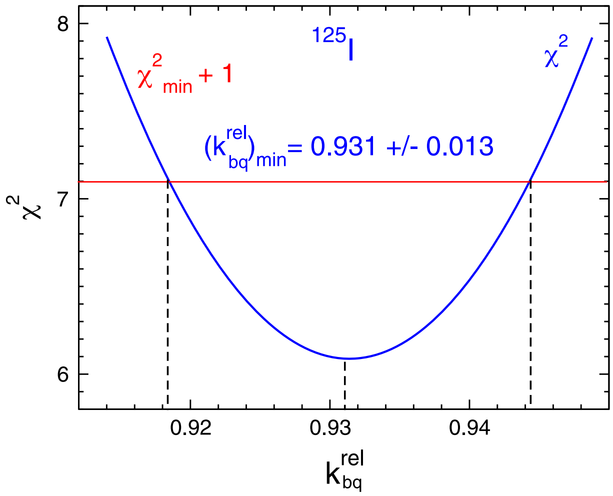

FIG. 1. Comparison between 25 measured DRCs for ^{125}I seed models using TLD and the respective Monte Carlo calculated value. $(k_{\mathrm{bq}}^{\mathrm{rel}})^{-1}$, consequently, has a value of 1.074 ± 0.015.

DRCs agree well with their new measured values for both seeds, and our revision of the previous measured DRC for the 6711 seed[30] now agrees better with their new measurement and with the calculated values.

4. CONCLUSIONS AND DISCUSSION

Important parameters in dosimetry at low energy (e.g., f^{rel}, $k_{\mathrm{bq}}^{\mathrm{rel}}$, P_{phant}) are now measured or calculated with higher accuracy and precision than in the past. This work has focused on calculating the phantom correction and the relative absorbed-dose energy dependence for the energy spectra generated by ^{125}I and ^{103}Pd brachytherapy seeds using a state-of-the-art tool for such calculations. Results show that the generalized value of 1.41 used as $S_{\mathrm{AD}}^{\mathrm{rel}}$ for ^{125}I and ^{103}Pd seed dose measurements needs to be updated. Small differences (≈±0.5%) have been detected in $S_{\mathrm{AD,med}}^{\mathrm{rel}}$ values for ^{125}I seed models containing silver vs those without silver (Table II) when using small chips, but differences are larger when using large chips and rods. Although these differences are small compared to the typical uncertainty in dose measurements at low energies, they have been included in this work.

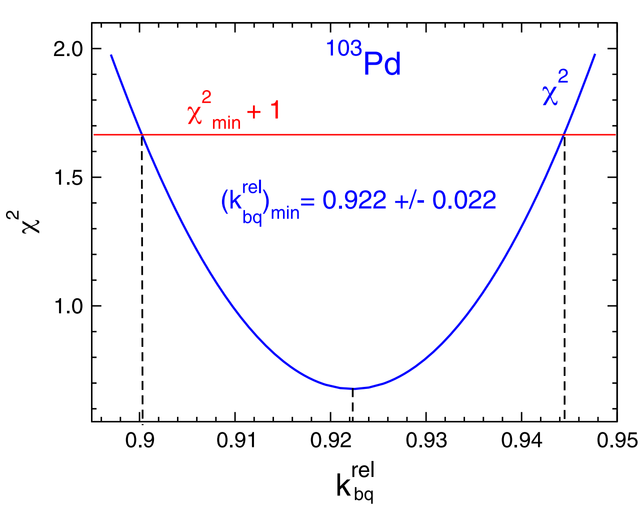

FIG. 2. Same as Fig. 1 but for six measured DRCs for ^{103}Pd seed models. $(k_{\mathrm{bq}}^{\mathrm{rel}})^{-1}$ is 1.084 ± 0.026.

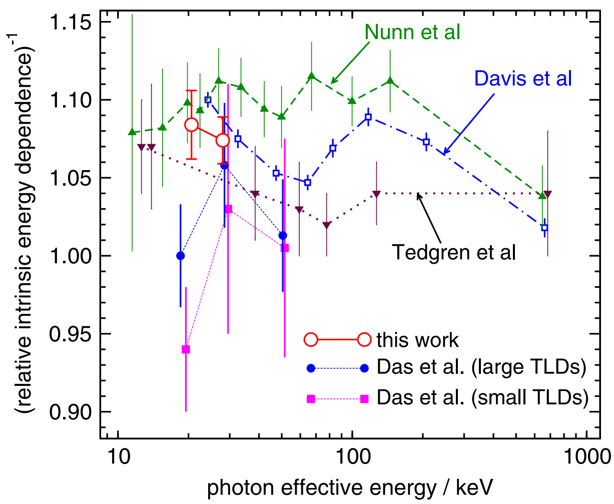

FIG. 3. Comparison of the inverse of the intrinsic energy dependence relative to high-energy beams, $(k_{\mathrm{bq}}^{\mathrm{rel}})^{-1}$, deduced here and as measured by other authors. The values found in this study agree reasonably with those values measured for x-ray beams by Davis *et al.* (Ref. 9), Nunn *et al.* (Ref. 10), and Tedgren *et al.* (Ref. 11). Das *et al.* (Ref. 18) reported an average value of 1.00, but the uncertainty in measurements is large compared to the others.

Based on the individual values on which values of Table II are based, variations in f^{rel} values of up to 3.6% for ^{125}I seeds and up to 5.6% for ^{103}Pd have been calculated amongst the most common TLD sizes used in brachytherapy dosimetry (3×3×1 and 1×1×1 mm^3 chips and 6 mm long by 1 mm diameter rods). Furthermore, for a given chip size, the f^{rel} values for ^{125}I and ^{103}Pd seed models differ from each other by up to 5.4%, 3.6%, and 6.5% for large chips, small chips, and rods, respectively, and it may be up to 8.4% among any TLD shape and seed model, i.e., one must use f^{rel} values specific to the seed and TLD shape involved. If we further take into account the difference in the relative intrinsic energy dependence, the overall relative absorbed-dose sensitivity values are as much as 4.2%, 2.8%, and 5.0% less for ^{103}Pd than for ^{125}I for the large chips, small chips, and rods, respectively. This finding is significant because to date the same value of the relative absorbed-dose sensitivity has been used to correct dose measurements for both ^{125}I and ^{103}Pd seed models and any shape of TLD. It was also shown that f^{rel} [as defined in Eqs. (3) and (9)] is similar for measurements in water or solid water, and it is assumed it does not change for other plastic phantoms either.

Phantom corrections for a given material are nearly the same for different seed models (range up to 0.7% in the worst case) but do depend on the isotope involved. Uncertainties in the phantom corrections from uncertainties in the composition and density dominate and are likely ≈3%.

Analysis of the calculated and measured data also shows that values of $(k_{\mathrm{bq}}^{\mathrm{rel}})^{-1}$ of TLDs for brachytherapy dose measurements are 1.074 and 1.084 for ^{125}I and ^{103}Pd seeds, respectively. Our values are in agreement with values measured by other authors for x-ray beams with similar mean

TABLE VII. Revised measured DRC values of ^{125}I and ^{103}Pd seed models. Λ_{MC} is the Monte Carlo calculated dose rate constant (column RR, Table VI). Λ_{meas}^{rev} is the revised measured DRC determined by replacing original S_{AD}^{rel} by $(f^{rel} \cdot k_{bq}^{rel})^{-1}$, found in this work (Tables IV and V and Figs. 1 and 2). Percentage uncertainty, s_m^{rev}, is determined as $s_m^{rev} = \sqrt{s_m''^2 + s_{k_{bq}}^2}$, where $s_{k_{bq}}$ is the percentage uncertainty of the relative intrinsic energy dependence, k_{bq}^{rel}, found in this work. Λ_{avg}^{rev} is the average of Λ_{MC} and Λ_{meas}^{rev} values, and Λ_{CON} is the DRC consensus value reported in TG-43U1 and TG-43U1S1. Last column shows difference between Monte Carlo and revised measured average values and the consensus values of DRCs of the ^{125}I and ^{103}Pd brachytherapy seed models currently in the market.

Seed model	Λ_{MC}[a]	$\Lambda_{meas}^{rev} \pm s_m^{rev}$	$[(\Lambda_{MC} - \Lambda_{meas}^{rev})/\Lambda_{meas}^{rev}]\%$	Λ_{avg}^{rev}	Λ_{CON}	$[(\Lambda_{CON} - \Lambda_{avg}^{rev})/\Lambda_{avg}^{rev}]\%$
^{103}Pd						
Theragenics 200	0.685	0.653 ± 7.8%	4.8	0.669	0.686	2.5
NASI MED3633	0.665	0.675 ± 5.3%	−1.5	0.670	0.688	2.7
Best 2335	0.654	0.673 ± 7.9%	−2.9	0.664	0.685	3.2
Draximage Pd-1	0.627	0.628 ± 7.3%	−0.2	0.628	—	—
Advantage IAPd-103	0.661	0.675 ± 7.3%	−2.1	0.668	—	—
InterSource IBT 1031L	0.663	0.658 ± 3.9%	0.8	0.660	—	—
			Ave = −0.2%			Ave = 2.8%
^{125}I						
GE 6711	0.928	0.915 ± 6.2%	1.4	0.921	0.965	4.7
Imagyn IS-12051	0.924	0.866 ± 8.0%	6.7	0.895	0.940	5.0
ProstaSeed SL-125	0.931	0.978 ± 3.5%	−4.8	0.955	0.953	−0.2
EchoSeed 6733	0.934	0.913 ± 6.4%	2.3	0.924	0.980	6.1
IsoAid IAI-125A	0.925	0.945 ± 5.9%	−2.2	0.935	0.981	4.9
Select Seed130.002	0.917	0.885 ± 6.3%	3.6	0.901	—	—
Implant Scie. 3500	0.987	0.983 ± 4.2%	−0.5	0.985	1.014	3.0
IsoSeed I12.S17	0.915	0.874 ± 5.1%	5.1	0.893	—	—
Theragenics AgX100	0.900	0.923 ± 5.4%	−2.5	0.911	—	—
PharmaSeed BT-125-1	0.906	0.880 ± 6.3%	2.9	0.893	—	—
Draximage LS-1	0.922	0.943 ± 5.1%	−2.2	0.933	0.972	4.2
Symmetra I25.S06	1.004	0.961 ± 6.0%	4.5	0.983	1.012	3.0
GE 6702	1.007	1.026 ± 3.6%	−1.8	1.016	1.036	1.9
NASI MED3631	0.995	1.032 ± 5.5%	−3.6	1.014	1.036	2.2
Best 2301	0.999	0.944 ± 7.0%	5.8	0.972	1.018	4.8
STM 1251	0.992	0.968 ± 6.4%	2.5	0.980	1.018	3.0
InterSource IBt 1251L	0.991	0.976 ± 5.7%	1.5	0.984	1.038	5.5
			Ave = 1.2%			Ave = 3.8%

[a]Uncertainty of Λ_{MC} is 1.5%.

energies[9–11] and with the value reported in Ref. 27 which is based on an unpublished result for ^{125}I seeds. Thus, significant changes are needed for that subset of previous experimental data that used calculated relative absorbed-dose energy dependence values to correct the measurements based on a relative intrinsic energy dependence of 1.0 .[18]

In general, the relative absorbed-dose sensitivity needs to be updated taking into account not only the application of the recently and more accurately measured intrinsic energy dependence value but also considering the f^{rel} dependence on TLD shape and seed model. The $S_{AD,med}^{rel}$ value can be determined using Eq. (8), the tabulated values of $(f^{rel})^{-1}$ and the values of k_{bq}^{rel} determined in Figs. 1 and 2. Compared to the oft-used value of 1.41 for $S_{AD,med}^{rel}$, our results imply typical values of 1.47 for ^{103}Pd seeds with (1 mm)^3 LiF TLDs and 1.46 and 1.51 for ^{125}I seeds using rods and (1 mm)^3 TLDs, respectively. Our calculated P_{phant} values also modify the DRCs by an average of 1.6% in the same direction for ^{103}Pd seeds and 0.7% in the opposite direction for ^{125}I seeds

TABLE VIII. Comparison of present results to those of Kennedy *et al.* (Ref. 27) for the THINSeed 9011 and GE 6711 ^{125}I seeds. Kennedy *et al.* used a value of $(k_{bq}^{rel})^{-1}$ = 1.092 ± 0.027 compared to the value 1.074 ± 0.015 presented here.

	Λ_{WAFAC} (calc) (cGy h^{-1} U^{-1})		Λ_{meas} (cGy h^{-1} U^{-1})	
Seed	Kennedy *et al.*	Present	Kennedy *et al.*	Present
9011	0.923 ± 0.004	0.930 ± 0.002[a]	0.940 ± 0.055	—
6711	0.921 ± 0.004	0.928 ± 0.002[a]	0.921 ± 0.055	0.915 ± 0.06[b]

[a]Statistical component of uncertainty only. Overall uncertainty ±1.5%.
[b]Revision of measurements by Dolan *et al.* (Ref. 30) (0.971 ± 6.1%).

which leads to the overall decreases in the DRCs of 4% and 6.4%, respectively for ^{103}Pd and ^{125}I seeds.

The discrepancy between the previous Monte Carlo calculated and measured DRC values caused the AAPM TG-43 to define a consensus value of the DRC of brachytherapy seed models as the average of the two data sets. However, this work finds that by applying the updated and appropriate relative absorbed-dose sensitivity to correct measurements at low energies, on average such differences decrease, and all individual cases agree within the uncertainties of the calculations and measurements. At present, the TG-43U1 (Ref. 2) and TG-43U1S1 (Ref. 12) consensus values are, on average, 2.8% and 3.8% higher than the average values of the revised and calculated values presented here for ^{103}Pd and ^{125}I seeds, respectively. The DRC scales the 3D dose distribution in a brachytherapy treatment plan, and the higher TG-43U1 and TG-43U1S1 values are overestimating the dose delivered to the patient by 3%–4% compared to the dose that would be given using the present results. Perhaps more importantly, in a worst case the dose delivered for two different model seeds would differ by up to 6.1% based on the use of the current consensus values vs the average revised values proposed here.

This work suggests that the dose rate constant consensus value reported by TG-43U1 or TG-43U1S1 for each brachytherapy seed model used clinically should be revised and updated to those determined by the average of values calculated by Monte Carlo simulation and values measured with the appropriate relative absorbed-dose sensitivity. Going one step further, given that,

- there is overall agreement between the measured and calculated DRCs,
- the overall uncertainty on the calculated DRCs, i.e., 1.5%, is considerably lower than that on the measured values,
- most measured DRCs are directly proportional to the MC calculated DRC through the phantom correction factor, and
- making accurate TLD measurements is almost impossible without relative absorbed-dose sensitivities which are specifically applicable to the annealing and readout protocols used,

one might suggest that the relevant committee consider adopting the Monte Carlo calculated values for clinical use rather than the averaged consensus values. This is already done for $g(r)$ and $F(r,\theta)$ values in LDR brachytherapy and for DRCs of HDR ^{192}Ir sources. In order to avoid possibly significant mistakes in modeling new seeds, a measured verification that the calculated DRCs are reasonable and/or a verification that the spectra from any new seed model agrees with measured spectra[40] would still be necessary before adopting the calculated DRC as the clinical value.

ACKNOWLEDGMENTS

The authors thank their Carleton colleague Martin Martinov for drawing attention to two further changes needed in seed models and for providing two more accurate calculated DRCs. The authors thank Steve Davis of McGill University for pointing out some inconsistencies in an early version of this paper and Mark Rivard of Tufts for helpful comments on an early version of the manuscript. The authors also thank Rowan Thomson of CLRP, Carleton University, for her continuing work in debugging the BrachyDose code. The authors thank Bob Wallace of Cedars-Sinai Medical Center and Zhonglu Wang of Saint Anne's Hospital/Nolan Hertel of Georgia Tech for information about their respective papers. Finally, the authors would like to thank the 9(sic!) separate journal reviewers/editors who helped us tighten up the manuscript. This work was supported by NSERC, the CRC program, CFI, and OIT.

[a)]Author to whom correspondence should be addressed. Electronic mail: manuel.rodriguez@rmp.uhn.ca

[1]R. Nath, L. L. Anderson, G. Luxton, K. A. Weaver, J. F. Williamson, and A. S. Meigooni, "Dosimetry of interstitial brachytherapy sources: Recommendations of the AAPM Radiation Therapy Committee Task Group No. 43," Med. Phys. **22**, 209–234 (1995).

[2]M. J. Rivard, B. M. Coursey, L. A. DeWerd, M. S. Huq, G. S. Ibbott, M. G. Mitch, R. Nath, and J. F. Williamson, "Update of AAPM Task Group No. 43 Report: A revised AAPM protocol for brachytherapy dose calculations," Med. Phys. **31**, 633–674 (2004).

[3]G. H. Hartmann, W. Schlegel, and H. Scharfenberg, "The three-dimensional dose distribution of ^{125}I seeds in tissue," Phys. Med. Biol. **28**, 693–699 (1983).

[4]K. A. Weaver, "Response of LiF powder to ^{125}I photons," Med. Phys. **11**, 850–854 (1984).

[5]K. A. Weaver, V. Smith, D. Huang, C. Barnett, M. C. Schell, and C. Ling, "Dose parameters of ^{125}I and ^{192}Ir seed sources," Med. Phys. **16**, 636–643 (1989).

[6]A. S. Meigooni, J. A. Meli, and R. Nath, "Influence of the variation of energy spectra with depth in the dosimetry of ^{192}Ir using LiF TLD," Phys. Med. Biol. **33**, 1159–1170 (1988).

[7]*Ibid.*, "A comparison of solid phantoms with water for dosimetry of ^{125}I brachytherapy sources," Med. Phys. **15**, 695–701 (1988).

[8]P. J. Muench, A. S. Meigooni, R. Nath, and W. L. McLaughlin, "Photon energy dependence of the sensitivity of radiochromic film and comparison with silver halide film and LiF TLDs used for brachytherapy dosimetry," Med. Phys. **18**, 769–775 (1991).

[9]S. D. Davis, C. K. Ross, P. N. Mobit, L. Van der Zwan, W. J. Chase, and K. R. Shortt, "The response of LiF TLDs to photon beams in the energy range from 30 kV to ^{60}Co γ-rays," Radiat. Prot. Dosim. **106**, 33–44 (2003).

[10]A. A. Nunn, S. D. Davis, J. A. Micka, and L. A. DeWerd, "LiF:Mg,Ti TLD response as a function of photon energy for moderately filtered x-ray spectra in the range of 20–250 kVp relative to ^{60}Co," Med. Phys. **35**, 1859–1869 (2008).

[11]A. C. Tedgren, A. Hedman, J.-E. Grindborg, and G. A. Carlsson, "Response of LiF:Mg,Ti thermoluminescent dosimeters at photon energies relevant to dosimetry of brachytherapy (<1 MeV)," Med. Phys. **38**, 5539–5550 (2011).

[12]M. J. Rivard, W. M. Butler, L. A. DeWerd, M. S. Huq, G. S. Ibbott, A. S. Meigooni, C. S. Melhus, M. G. Mitch, R. Nath, and J. F. Williamson, "Supplement to the 2004 update of the AAPM Task Group No. 43 Report," Med. Phys. **34**, 2187–2205 (2007).

[13]Y. S. Horowitz, "Update on AAPM Task Group No. 43 Report—Brachytherapy and TLD," Radiat. Prot. Dosim. **133**, 124–125 (2009).

[14]Q. Liang, S. D. Davis, Y. S. Horowitz, and L. A. DeWerd, "Investigation of the relative TL response for low-energy X-rays relative to ^{60}Co for TLD-100," Radiat. Meas. **46**, 1453–1456 (2011).

[15]D. W. O. Rogers, "General characteristics of radiation dosimeters and a terminology to describe them," in *Clinical Dosimetry Measurements in*

Radiotherapy, edited by D. W. O. Rogers and J. E. Cygler (Medical Physics Publishing, Madison, Wisconsin, 2009), pp. 137–145.

[16]P. R. Almond, P. J. Biggs, B. M. Coursey, W. F. Hanson, M. S. Huq, R. Nath, and D. W. O. Rogers, "The AAPM's TG-51 protocol for clinical reference dosimetry of high-energy photon and electron beams," Med. Phys. **26**, 1847–1870 (1999).

[17]J. F. Williamson and M. J. Rivard, "Thermoluminescent detector and Monte Carlo techniques for reference-quality brachytherapy dosimetry," in *Clinical Dosimetry Measurements in Radiotherapy*, edited by D. W. O. Rogers and J. E. Cygler (Medical Physics Publishing, Madison, Wisconsin, 2009), pp. 437–499.

[18]R. K. Das, Z. Li, H. Perera, and J. F. Williamson, "Accuracy of Monte Carlo photon transport simulation in characterizing brachytherapy dosimeter energy-response artefacts," Phys. Med. Biol. **41**, 995–1006 (1996).

[19]T. Budd, M. Marshall, L. H. J. Peaple, and J. A. Douglas, "The low- and high-temperature response of lithium fluoride dosemeters to X-rays," Phys. Med. Biol. **24**, 71–80 (1979).

[20]T. Kron, L. Duggan, T. Smith, A. Rosenfeld, M. Butson, G. Kaplan, S. Howlett, and K. Hyodo, "Dose response of various radiation detectors to synchrotron radiation," Phys. Med. Biol. **43**, 3235–3259 (1998).

[21]P. Olko, P. Bilski, and J.-L. Kim, "Microdosimetric interpretation of the photon energy response of LiF:Mg,Ti detectors," Radiat. Prot. Dosim. **100**, 119–122 (2002).

[22]A. S. Meigooni, V. Mishra, H. Panth, and J. Williamson, "Instrumentation and dosimeter-size artifacts in quantitative thermoluminescence dosimetry of low-dose fields," Med. Phys. **22**, 555–561 (1995).

[23]J. A. Meyer, J. R. Palta, and K. R. Hogstrom, "Demonstration of relatively new electron dosimetry measurement techniques on the Mevatron 80," Med. Phys. **11**, 670–677 (1984).

[24]AAPM TG–21, "A protocol for the determination of absorbed dose from high-energy photon and electron beams," Med. Phys. **10**, 741–771 (1983).

[25]S. M. Seltzer and P. M. Bergstrom, "Changes in the U.S. primary standards for the air kerma from gamma-ray beams," J. Res. Natl. Inst. Stand. Technol. **108**, 359–381 (2003).

[26]S. M. Seltzer, P. J. Lamperti, R. Loevinger, M. G. Mitch, J. T. Weaver, and B. M. Coursey, "New national air-kerma-strength standards for ^{125}I and ^{103}Pd brachytherapy seeds," J. Res. Natl. Inst. Stand. Technol. **108**, 337–358 (2003).

[27]R. M. Kennedy, S. D. Davis, J. A. Micka, and L. A. DeWerd, "Experimental and Monte Carlo determination of the TG-43 dosimetric parameters for the model 9011 THINSeed brachytherapy source," Med. Phys. **37**, 1681–1688 (2010).

[28]P. Mobit and I. Badragan, "Response of LiF-TLD micro-rods around ^{125}I radioactive seed," Phys. Med. Biol. **48**, 3129–3142 (2003).

[29]N. S. Patel, S.-T. Chiu-Tsao, J. F. Williamson, P. Fan, T. Duckworth, D. Shasha, and L. B. Harrison, "Thermoluminescent dosimetry of the Symmetra ^{125}I model I25.S06 interstitial brachytherapy seed," Med. Phys. **28**, 1761–1769 (2001).

[30]J. Dolan, Z. Li, and J. F. Williamson, "Monte Carlo and experimental dosimetry of an ^{125}I brachytherapy seed," Med. Phys. **33**, 4675–4684 (2006).

[31]R. M. Harrison, "Tissue–air ratios and scatter–air ratios for diagnostic radiology (1–4 mm Al HVL)," Phys. Med. Biol. **28**, 1–18 (1983).

[32]I. Kawrakow, "Accurate condensed history Monte Carlo simulation of electron transport. I. EGSnrc, the new EGS4 version," Med. Phys. **27**, 485–498 (2000).

[33]I. Kawrakow and D. W. O. Rogers, "The EGSnrc code system: Monte Carlo simulation of electron and photon transport," Technical Report PIRS-701, National Research Council of Canada, Ottawa, Canada, 2000 [http://www.nrc-cnrc.gc.ca/eng/solutions/advisory/egsnrc/download_egsnrc.html].

[34]G. Yegin and D. W. O. Rogers, "A fast Monte Carlo code for multi-seed brachytherapy treatments including interseed effects," Med. Phys. **31**, 1771 (2004), abstract.

[35]R. E. P. Taylor, G. Yegin, and D. W. O. Rogers, "Benchmarking BrachyDose: Voxel-based EGSnrc Monte Carlo calculations of TG-43 dosimetry parameters," Med. Phys. **34**, 445–457 (2007).

[36]R. M. Thomson, G. Yegin, R. E. P. Taylor, J. G. H. Sutherland, and D. W. O. Rogers, "Fast Monte Carlo dose calculations for brachytherapy with BrachyDose," Med. Phys. **37**, 3910–3911 (2010), abstract.

[37]Z. J. Chen and R. Nath, "Photon spectrometry for the determination of the dose-rate constant of low-energy photon-emitting brachytherapy sources," Med. Phys. **34**, 1412–1430 (2007).

[38]Z. Chen and R. Nath, "A systematic evaluation of the dose-rate constant determined by photon spectrometry for 21 different models of low-energy photon-emitting brachytherapy sources," Phys. Med. Biol. **55**, 6089–6104 (2010).

[39]J. Usher-Moga, S. M. Beach, and L. A. DeWerd, "Spectroscopic output of ^{125}I and ^{103}Pd low dose rate brachytherapy sources," Med. Phys. **36**, 270–278 (2009).

[40]M. Rodriguez and D. W. O. Rogers, "On determining dose rate constants spectroscopically," Med. Phys. **40**, 011713 (10pp.) (2013).

[41]M. R. McEwen and D. Niven, "Characterization of the phantom material virtual water in high-energy photon and electron beams," Med. Phys. **33**, 876–887 (2006).

[42]K.-P. Hermann, L. Geworski, M. Muth, and D. Harder, "Polyethylene-based water-equivalent phantom material for x-ray dosimetry and tube voltages from 10 to 100 kV," Phys. Med. Biol. **30**, 1195–1200 (1985).

[43]D. Duggan and B. L. Johnson, "Dosimetry of the I-Plant Model 3500 iodine-125 brachytherapy source," Med. Phys. **28**, 661–670 (2001).

[44]Z. Wang and N. Hertel, "Determination of dosimetric characteristics of OptiSeed a plastic brachytherapy ^{103}Pd source," Appl. Radiat. Isot. **63**, 311–321 (2005).

[45]S. Chiu-Tsao, T. L. Duckworth, C. Hsiung, Z. Li, J. Williamson, N. Patel, and L. B. Harrison, "Thermoluminescent dosimetry of the SourceTech Medical model STM1251 ^{125}I seed," Med. Phys. **30**, 1732–1735 (2003).

[46]M. J. Berger and J. H. Hubbell, "XCOM: Photon cross sections on a personal computer," Report NBSIR87-3597 (National Institute of Standards Technology (NIST), Gaithersburg, MD 20899, 1987).

[47]B. Walters, I. Kawrakow, and D. W. O. Rogers, "DOSXYZnrc Users Manual," NRC Technical Report PIRS-794revB (National Research Council Canada, Ottawa, Canada, 2011), http://www.nrc-cnrc.gc.ca/eng/solutions/advisory/beam/download_beam.html.

[48]G. Mora, A. Maio, and D. W. O. Rogers, "Monte Carlo simulation of a typical ^{60}Co therapy source," Med. Phys. **26**, 2494–2502 (1999).

[49]D. Sheikh-Bagheri and D. W. O. Rogers, "Monte Carlo calculation of nine megavoltage photon beam spectra using the BEAM code," Med. Phys. **29**, 391–402 (2002).

[50]G. Anagnostopoulos, D. Baltas, P. Karaiskos, P. Sandilos, P. Papagiannis, and L. Sakelliou, "Thermoluminescent dosimetry of the selectSeed ^{125}I interstitial brachytherapy seed," Med. Phys. **29**, 709–716 (2002).

[51]P. Papagiannis, L. Sakelliou, G. Anagnostopoulos, and D. Baltas, "On the dose rate constant of the selectSeed ^{125}I interstitial brachytherapy seed," Med. Phys. **33**, 1522–1523 (2006).

[52]Z. Li, J. J. Fan, and J. R. Palta, "Experimental measurements of dosimetric parameters on the transverse axis of a new ^{125}I source," Med. Phys. **27**, 1275–1280 (2000).

[53]D. W. O. Rogers, "Analytic and graphical methods for assigning errors to parameters in non-linear least squares fitting," Nucl. Instrum. Methods **127**, 253–260 (1975).

[54]R. E. P. Taylor and D. W. O. Rogers, "An EGSnrc Monte Carlo-calculated database of TG-43 parameters," Med. Phys. **35**, 4228–4241 (2008).

[55]J. F. Williamson, "Dosimetric characteristics of the DRAXIMAGE model LS-1 interstitial brachytherapy source design: A Monte Carlo investigation," Med. Phys. **29**, 509–521 (2002).

[56]T. D. Bohm, P. M. DeLuca, Jr., and L. A. DeWerd, "Brachytherapy dosimetry of ^{125}I and ^{103}Pd sources using an updated cross section library for the MCNP Monte Carlo transport code," Med. Phys. **30**, 701–711 (2003).

[57]J. J. DeMarco, R. E. Wallace, and K. Boedeker, "An analysis of MCNP cross-sections and tally methods for low-energy photon emitters," Phys. Med. Biol. **47**, 1321–1332 (2002).

[58]H. Hedtjärn, G. A. Carlsson, and J. F. Williamson, "Monte Carlo-aided dosimetry of the symmetra model I25.S06 I^{125}, interstitial brachytherapy seed," Med. Phys. **27**, 1076–1085 (2000).

[59]J. F. Williamson, B. M. Coursey, L. A. DeWerd, W. F. Hanson, R. Nath, and G. Ibbott, "Guidance to users of Nycomed Amersham and North American Scientific, Inc., I-125 Interstitial Sources: Dosimetry and calibration changes: Recommendations of the AAPM Radiation Therapy Committee Ad Hoc Subcommittee on low-energy seed dosimetry," Med. Phys. **26**, 570–573 (1999).

[60]M. J. Rivard, "A discretized approach to determining TG-43 brachytherapy dosimetry parameters: Case study using Monte Carlo calculations for the MED3633 ^{103}Pd source," Appl. Radiat. Isot. **55**, 775–782 (2001).

[61]V. M. Tello, R. C. Tailor, and W. F. Hanson, "How water equivalent are water-equivalent solid materials for output calibration of photon and electron beams?," Med. Phys. **22**, 1177–1189 (1995).

[62]IAEA, in *Absorbed Dose Determination in External Beam Radiotherapy: An International Code of Practice for Dosimetry Based on Standards of Absorbed Dose to Water*, Technical Report Series Vol. 398 (IAEA, Vienna, 2001).
[63]ICRU, "Tissue substitutes in radiation dosimetry and measurements," ICRU Report 44 (ICRU, Washington, DC, 1989).
[64]A. S. Meigooni, Z. Li, V. Mishra, and J. F. Williamson, "A comparative study of dosimetric properties of plastic water and solid water in brachytherapy applications," Med. Phys. **21**, 1983–1987 (1994).
[65]J. F. Williamson, "Comparison of measured and calculated dose rates in water near I-125 and Ir-192 seeds," Med. Phys. **18**, 776–786 (1991).
[66]G. Luxton, "Comparison of radiation-dosimetry in water and in solid phantom materials for I-125 and Pd-103 brachytherapy sources—EGS4 Monte Carlo study," Med. Phys. **21**, 621–641 (1994).
[67]L. A. Buckley, B. R. Thomadsen, and L. A. DeWerd, "The water-equivalence of phantom materials for ^{90}Sr–^{90}Y beta particles," Med. Phys. **28**, 1010–1015 (2001).
[68]D. M. Gearheart, A. Drogin, K. Sowards, A. Meigooni, and G. S. Ibbott, "Dosimetric characteristics of a new ^{125}I brachytherapy source," Med. Phys. **27**, 2278–2285 (2000).
[69]A. S. Meigooni, J. L. Hayes, H. Zhang, and K. Sowards, "Experimental and theoretical determination of dosimetric characteristics of IsoAid ADVANTAGE™ ^{125}I brachytherapy source," Med. Phys. **29**, 2152–2158 (2002).
[70]Z. Chen, P. Bongiorni, and R. Nath, "Experimental characterization of the dosimetric properties of a newly desined I-Seed model AgX100 ^{125}I interstitial brachytherapy source," Brachytherapy **11**, 476–482 (2012).
[71]C. C. Popescu, J. Wise, K. Sowards, A. S. Meigooni, and G. S. Ibbott, "Dosimetric characteristics of the PharmaSeed model BT-125-1 source," Med. Phys. **27**, 2174–2181 (2000).
[72]A. S. Meigooni, D. M. Gearheart, and K. Sowards, "Experimental determination of dosimetric characteristics of best ^{125}I brachytherapy source," Med. Phys. **27**, 2168–2173 (2000).
[73]R. Nath and N. Yue, "Dosimetric characterization of an encapsulated interstitial brachytherapy source of ^{125}I on a tungsten substrate," Brachytherapy **1**, 102–109 (2002).
[74]R. E. Wallace, "Empirical dosimetric characterization of model I125-SL ^{125}Iodine brachytherapy source in phantom," Med. Phys. **27**, 2796–2802 (2000).
[75]Z. Chen and R. Nath, "Dose rate constant and energy spectrum of interstitial brachytherapy sources," Med. Phys. **28**, 86–96 (2001).
[76]J. I. Monroe and J. F. Williamson, "Monte Carlo-aided dosimetry of the Theragenics TheraSeed Model 200 ^{103}Pd interstitial brachytherapy seed," Med. Phys. **29**, 609–621 (2002).
[77]R. Nath, N. Yue, K. Shahnazi, and P. Bongiorini, "Measurement of dose-rate constant for ^{103}Pd seeds with air kerma strength calibration based upon a primary national standard," Med. Phys. **27**, 655–658 (2000).
[78]Z. Li, J. R. Palta, and J. J. Fan, "Monte Carlo caculations and experimental measurements of dosimetry parameters of a new ^{103}Pd source," Med. Phys. **27**, 1108–1112 (2000).
[79]R. E. Wallace and J. J. Fan, "Dosimteric characterization of a new design ^{103}Pd brachytherapy source," Med. Phys. **26**, 2465–2470 (1999).
[80]S. Bernard and S. Vynckier, "Dosimetric study of a new polymer encapsulated ^{103}Pd seed," Phys. Med. Biol. **50**, 1493–1504 (2005).
[81]A. S. Meigooni, Z. Bharucha, M. Yoe-Sein, and K. Sowards, "Dosimetric characteristics of the Best double-wall ^{103}Pd brachytherapy source," Med. Phys. **28**, 2567–2575 (2001).
[82]S. W. Peterson and B. Thomadsen, "Measurements of the dosimetric constants for a new ^{103}Pd brachytherapy source," Brachytherapy **1**, 110–119 (2002).
[83]A. S. Meigooni, H. Zhang, C. Perry, S. A. Dini, and R. A. Koona, "Theoretical and experimental determination of dosimetric characteristics for brachyseed Pd-103, model Pd-1, source," Appl. Radiat. Isot. **58**, 533–541 (2003).
[84]R. Nath, N. Yue, and E. Roa, "Experimental determination of dosimetric characterization of a newly designed encapsulated interstitial brachytherapy source of ^{103}Pd-model Pd-1," Med. Phys. **29**, 2433–2434 (2002).
[85]A. S. Meigooni, S. A. Dini, S. B. Awan, K. Dou, and R. A. Koona, "Theoretical and experimental determination of dosimetric characterictics for ADVANTAGE Pd-103 brachytherapy source," Appl. Radiat. Isot. **64**, 881–887 (2006).
[86]A. S. Meigooni, K. Sowards, and M. Soldano, "Dosimetric characteristics of InterSource^{103} palladium brachytherapy source," Med. Phys. **27**, 1093–1100 (2000).
[87]G. S. Ibbott and R. Nath, "Dose-rate constant for Imagyn ^{125}I brachytherapy source," Med. Phys. **28**, 705 (2001).
[88]R. Nath and N. Yue, "Dose distribution along the transverse axis of a new ^{125}I source for interstitial brachytherapy," Med. Phys. **27**, 2536–2540 (2000).
[89]Z. Li, "Monte Carlo calculations of dosimetry parameters of the Urocor Prostaseed ^{125}I source," Med. Phys. **29**, 1029–1034 (2002).
[90]K. Sowards and A. S. Meigooni, "A Monte Carlo evaluation of the dosimetric characteristics of the EchoSeed™ Model 6733 ^{125}I brachytherapy source," Brachytherapy **1**, 227–232 (2002).
[91]A. S. Meigooni, S. A. Dini, K. Sowards, J. L. Hayes, and A. Al-Otoom, "Experimental determination of the TG-43 dosimetric characteristics of EchoSeed model 6733 ^{125}I brachytherapy source," Med. Phys. **29**, 939–942 (2002).
[92]T. D. Solberg, J. J. DeMarco, G. Hugo, and R. E. Wallace, "Dosimetric parameters of three new solid core I-125 brachytherapy sources," J. Appl. Clin. Med. Phys. **3**, 119–134 (2002).
[93]M. J. Rivard, "Comprehensive Monte Carlo calculations of AAPM Task Group Report No. 43 dosimetry parameters for the Model 3500 I-Plant ^{125}I brachytherapy source," Appl. Radiat. Isot. **57**, 381–389 (2002).
[94]R. E. Wallace, "Model 3500 ^{125}I brachytherapy source dosimetric characterization," Appl. Radiat. Isot. **56**, 581–587 (2002).
[95]G. Lymperopoulou, P. Papagiannis, A. Angelopoulos, L. Sakelliou, P. Karaiskos, P. Sandilos, A. Przykutta, and D. Baltas, "Monte Carlo and thermoluminescence dosimetry of the new IsoSeed model I125.S17 ^{125}I interstitial brachytherapy seed," Med. Phys. **32**, 3313–3317 (2005).
[96]E. Pantelis, D. Baltas, E. Georgiou, P. Karaiskos, G. Lymperopoulou, P. Papariannis, L. Sakelliou, I. Seimenis, and E. Stilliaris, "Dose characterization of the new Bebig IsoSeed I25.S17 using polymer gel and MRI," Nucl. Instrum. Methods Phys. Res., Sect. A **569**, 529–532 (2006).
[97]F. Mourtada, J. Mikell, and G. Ibbott, "Monte Carlo calculations of AAPM Task Group Report No. 43 dosimetry parameters for the ^{125}I I-Seed AgX100 source model," Brachytherapy **11**, 237–244 (2012).
[98]R. Nath and N. Yue, "Experimental determination of a newly designed encapsulated interstitial brachytherapy source of iodine-125-model LS-1 BrachySeed," Appl. Radiat. Isot. **55**, 813–821 (2001).
[99]J. F. Williamson and F. J. Quintero, "Theoretical evaluation of dose distributions in water models 6711 and 6702 ^{125}I seeds," Med. Phys. **15**, 891–897 (1988).
[100]R. E. Wallace and J. J. Fan, "Report on the dosimetry of a new design ^{125}Iodine brachytherapy source," Med. Phys. **26**, 1925–1931 (1999).
[101]Z. Li and J. F. Williamson, "Measured transverse-axis dosimetric parameters of the model STM1251 ^{125}I interstitial source," J. Appl. Clin. Med. Phys. **3**, 212–217 (2002).
[102]A. S. Meigooni, M. M. Yoe-Sein, A. Y. Al-Otoom, and K. Sowards, "Determination of the dosimetric characteristics of InterSource ^{125}I brachytherapy source," Int. J. Appl. Radiat. Isot. **56**, 589–599 (2002).
[103]B. Reniers, S. Vynckier, and P. Scalliet, "Dosimetric study of the new InterSource^{125} iodine seed," Med. Phys. **28**, 2285–2299 (2001).
[104]R. E. Wallace (private communication, 2014).
[105]Z. Wang and N. Hertel (private communication, 2014).
[106]M. Martinov (personal communication, 2014).